Published article:

Hussein, MS, Lesnic, D and Ivanchov, MI (2014) *Simultaneous determination of time-dependent coefficients in the heat equation.* Computers and Mathematics with Applications, 67 (5). 1065 - 1091. ISSN 0898-1221

http://dx.doi.org/10.1016/j.camwa.2014.01.004

Simultaneous determination of time-dependent coefficients in the heat equation

M.S. Hussein[1,2], D. Lesnic[1] and M.I. Ivanchov[3]
[1] *Department of Applied Mathematics, University of Leeds, Leeds LS2 9JT, UK*
[2] *Department of Mathematics, College of Science, University of Baghdad, Al-jaderia, Baghdad, Iraq*
[3] *Faculty of Mechanics and Mathematics, Department of Differential Equations, Ivan Franko National University of Lviv, 1, Universytetska str., Lviv, 79000, Ukraine*
E-mails: mmmsh@leeds.ac.uk (M.S. Hussein), amt5ld@maths.leeds.ac.uk (D. Lesnic), ivanchov@franko.lviv.ua (M.I. Ivanchov).

Abstract
In this paper, the determination of time-dependent leading and lower-order thermal coefficients is investigated. We consider the inverse and ill-posed nonlinear problems of simultaneous identification of a couple of these coefficients in the one-dimensional heat equation from Cauchy boundary data. Unique solvability theorems of these inverse problems are supplied and, in one new case where they were not previously provided, are rigorously proved. However, since the problems are still ill-posed the solution needs to be regularized. Therefore, in order to obtain a stable solution, a regularized nonlinear least-squares objective function is minimized in order to retrieve the unknown coefficients. The stability of numerical results is investigated for several test examples with respect to different noise levels and for various regularization parameters. This study will be significant to researchers working on computational and mathematical methods for solving inverse coefficient identification problems with applications in heat transfer and porous media.

Keywords: Inverse problems; Thermal properties; Nonlinear optimization.

1 Introduction

Simultaneous determination of several unknown coefficients in parabolic partial differential equations has been investigated in various studies in the past, see e.g. the monographs of Prilepko et al. [27] and Ivanchov [17]. In heat conduction for example, attention was paid to the unique solvability of one-dimensional inverse problems for the heat equation in the case when the unknown thermal coefficients are constant [4], time-dependent [15, 16], space-dependent [1], or temperature-dependent, [20, 23, 24]. In these papers, the authors investigated the existence and uniqueness of solution of the inverse problem, though no numerical method/solution was presented.

When solving an inverse problem the choice of additional information about the solution is crucial since this information enables us to determine the unknown parameters of the process under consideration uniquely. Usually, this additional information/observation is given by the boundary conditions or, the value of the solution on a specific subdomain or, at a certain time, [19]. In [28], the authors proposed a new algorithm based on space decomposition in a reproducing kernel space for solving the inverse problem of finding the time-dependent thermal diffusivity. In [14, 18] the problem of finding the time-dependent leading coefficient and temperature distribution with Dirichlet boundary conditions and measured heat flux as overdetermination condition was considered. In [10], the author considered retrieving lower-order time-dependent coefficients using the Trace Type Functional approach, [5], which assumes that the governing partial differential equation is valid at the boundary. However, this approach does not seem so stable [11], and it has never been applied to inverse coefficient identification problems in which the unknown coefficients appear at the leading order in the heat operator.

In this paper, we investigate the inverse problems of simultaneous determination of time-dependent leading and lower-order thermal coefficients. The paper is organized as follows. In the next section, we give the mathematical formulations of three inverse problems for which the unique solvability theorems of [14, 15] are stated and, it one case, proved. The numerical finite-difference discretisation of the direct problem is described in Section 3, whilst Section 4 introduces the regularized nonlinear minimization used for solving in a stable manner the inverse problems under investigation. In Section 5, we provide numerical results and discussion. Finally, conclusions are presented in Section 6.

2 Mathematical Formulations of the Inverse Problems

Consider the linear one-dimensional parabolic equation with time-dependent coefficients

$$C(t)\frac{\partial u}{\partial t}(x,t) = K(t)\frac{\partial^2 u}{\partial x^2}(x,t) + Q(t)\frac{\partial u}{\partial x}(x,t), \qquad (x,t) \in (0,\ell) \times (0,T) =: \Omega \qquad (1)$$

where, in heat conduction, u represents the temperature in a finite slab of length $\ell > 0$ recorded over the time interval $(0, T)$ with $T > 0$, C and K represent the heat capacity and thermal conductivity of the heat conductor, respectively, $Q(t) = c(t)v(t)$ with c and v representing the heat capacity and velocity of a fluid flowing through the heat conducting body, [2, 9]. The first term in the right-hand side of equation (1) represents the diffusion, whilst the second term, if $v(t)$ is positive, represents the convection. A similar situation occurs in porous media, [7], where the properties are referred to as hydraulic rather than thermal as in heat transfer. For example, in the contaminant transport in groundwater the first term in the right-hand side of equation (1) represents the dispersion of contaminant as it moves through the porous medium, whilst the second term with $v(t)$ negative describes the advection of contaminant which flows along with the bulk movement of groundwater.

The initial condition is

$$u(x,0) = \phi(x), \qquad x \in [0,\ell], \qquad (2)$$

and the boundary and over-determination conditions are

$$u(0,t) = \mu_1(t), \qquad u(\ell,t) = \mu_2(t), \qquad t \in [0,T], \qquad (3)$$

$$-K(t)u_x(0,t) = \nu_1(t), \qquad K(t)u_x(\ell,t) = \nu_2(t), \qquad t \in [0,T]. \qquad (4)$$

Conditions (3) and (4) represent the specification of the boundary temperature and heat flux, respectively. Together they represent the Cauchy data for the inverse coefficient identification problems (ICIP) which are described next.

We distinguish three ICIPs covering the simultaneous determination of a couple of coefficients in (1). The case of identifying all three coefficients in (1) is deferred to a future work.

2.1 Inverse Problem 1

Assuming that $c(t)v(t) = 0$, the inverse problem 1 (IP1) requires the simultaneous determination of the time-dependent thermal conductivity $K(t) > 0$, the heat capacity $C(t) > 0$ and the temperature $u(x,t)$ satisfying the one-dimensional heat equation

$$C(t)\frac{\partial u}{\partial t}(x,t) = K(t)\frac{\partial^2 u}{\partial x^2}(x,t), \qquad (x,t) \in \Omega \tag{5}$$

subject to the initial and boundary conditions (2)–(4).

For this IP1 we have the following existence and uniqueness of solution theorems, [15].

Theorem 1. (Existence)
Suppose that:

1. *$\phi \in C^2[0,\ell]$ and μ_i, $\nu_i \in C^1[0,T]$ for $i = 1,2$.*
2. *The consistency conditions are satisfied:*

$$\mu_1(0) = \phi(0), \quad \mu_2(0) = \phi(\ell), \quad -\nu_1(0)\phi'(\ell) = \nu_2(0)\phi'(0), \quad \mu_1'(0)\phi''(\ell) = \mu_2'(0)\phi''(0).$$

3. *The following conditions are satisfied:*

$$\phi'(x) \geq 0, \quad x \in [0,\ell], \quad \phi''(x) + \phi''(\ell - x) > 0, \quad x \in [0,\ell/2),$$

$$\nu_1^2(t) + \nu_2^2(t) > 0, \quad \mu_2'(t) - \mu_1'(t) \geq 0, \quad (1+\chi(t))\,\mu_1'(t) + (1-\chi(t))\,\mu_2'(t) > 0,$$

$$\chi(t) > 0, \quad \chi'(t) \geq 0, \quad t \in [0,T],$$

$$(1+\chi(t))\,\phi''(x) + (1-\chi(t))\,\phi''(\ell - x) > 0, \quad x \in [0,\ell/2],\ t \in [0,T],$$

$$\phi''(x) - \phi''(\ell - x) \geq 0, \quad \text{or} \quad \phi''(x) - \phi''(\ell - x) \leq 0, \quad x \in [0,\ell/2],$$

where $\chi(t) = \frac{\nu_2(t)+\nu_1(t)}{\nu_1(t)-\nu_2(t)}$. Then, for a sufficiently small $T > 0$, the inverse problem (2)–(5) has at least one solution $\{C(t), K(t), u(x,t)\}$, where the functions $C(t)$ and $K(t)$ are continuous and positive on $[0,T]$ and $u(x,t)$ belongs to the class $C^{2,1}(\Omega) \cap C^{1,0}(\overline{\Omega})$.

Theorem 2. (Uniqueness)
Suppose that the following conditions are satisfied:

1. *$\phi \in C^2[0,\ell]$, $\mu_i \in C^1[0,T]$ and $\nu_i \in C[0,T]$ for $i = 1,2$;*
2. *$\phi''(x) \geq 0$ for $x \in [0,\ell]$, $\phi''(0) > 0$, $\mu_1'(t) > 0$, $\mu_2'(t) > 0$, $\nu_1(t) < 0$, $\nu_2(t) > 0$ for $t \in [0,T]$.*

If $\{C_j(t), K_j(t), u_j(x,t)\}$ for $j = 1,2$, are two solutions to the problem (2)–(5) such that $a_j(t) = K_j(t)/C_i(t)$ are piecewise analytic functions on $(0,T)$, then these solutions must coincide.

2.2 Inverse Problem 2

Assuming that $K(t) > 0$ is known, we now wish to determine the time-dependent heat capacity $C(t) > 0$, the convection/advection coefficient $Q(t)$ and the temperature $u(x,t)$ satisfying equations (1)–(4). By dividing (1) with $C(t)$ and denoting with $a(t) := K(t)/C(t)$ the thermal diffusivity and $b(t) := Q(t)/C(t)$, we obtain

$$\frac{\partial u}{\partial t}(x,t) = a(t)\frac{\partial^2 u}{\partial x^2}(x,t) + b(t)\frac{\partial u}{\partial x}(x,t), \qquad (x,t) \in \Omega. \tag{6}$$

For simplicity, since $K(t) > 0$ is known we can divide with it in (4) and denote the right hand sides by

$$-u_x(0,t) = \nu_1(t)/K(t) =: \overline{\nu}_1(t), \quad u_x(\ell,t) = \nu_2(t)/K(t) =: \overline{\nu}_2(t), \quad t \in [0,T]. \tag{7}$$

For this inverse problem 2 (IP2), we have the existence and uniqueness of solution Theorems 3 and 4 below, [16]. These are actually given for the more general reaction-convection-diffusion equation with a source term, namely,

$$\frac{\partial u}{\partial t}(x,t) = a(t)\frac{\partial^2 u}{\partial x^2}(x,t) + b(t)\frac{\partial u}{\partial x}(x,t) + d(x,t)u + f(x,t), \quad (x,t) \in \Omega, \tag{8}$$

where d and f are some given functions representing the reaction rate and source term, respectively. The triplet $(a(t), b(t), u(x,t))$ is called a solution to the IP2 given by equations (2), (3), (7) and (8) if it satisfies these equations and it belongs to the class $(H^{\gamma/2}[0,T])^2 \times H^{2+\gamma,1+\gamma/2}(\overline{\Omega})$ for some $\gamma \in (0,1)$, and $a(t) > 0$ for all $t \in [0,T]$. For the definition of the Hölder space, as well as other spaces of functions involved, see [21].

Theorem 3. (Existence)
Suppose that the following conditions are satisfied:

1. $\phi \in H^{2+\gamma}[0,\ell]$, μ_i, $\overline{\nu}_i \in H^{1+\gamma/2}[0,T]$ *for* $i = 1,2$, *and* d, f, $d_x, f_x \in H^{\gamma,\gamma/2}(\overline{\Omega})$;
2. $(\mu_1'(t) - f(0,t) - d(0,t)\mu_1(t))\overline{\nu}_2(t) + (\mu_2'(t) - f(\ell,t) - d(\ell,t)\mu_2(t))\overline{\nu}_1(t) > 0, \overline{\nu}_1(t) \geq 0$, $\overline{\nu}_2(t) \geq 0$, $\overline{\nu}_2(t) + \overline{\nu}_1(t) > 0$, $t \in [0,T]$, *and* $\phi''(x) > 0$, $x \in [0,\ell]$;
3. $\mu_1(0) = \phi(0)$, $\mu_2(0) = \phi(\ell)$, $-\overline{\nu}_1(0) = \phi'(0)$, *and* $\overline{\nu}_2(0) = \phi'(\ell)$.

Then the problem (2), (3), (7) and (8) has a (local) solution for $x \in [0,\ell]$ *and* $t \in [0,t_0]$, *where the time* $t_0 \in (0,T]$, *is determined by the input data of the problem.*

Theorem 4. (Uniqueness)
Suppose that the following condition is satisfied:

$$(\mu_1'(t) - f(0,t) - d(0,t)\mu_1(t))\overline{\nu}_2(t) + (\mu_2'(t) - f(\ell,t) - d(\ell,t)\mu_2(t))\overline{\nu}_1(t) \neq 0, \quad t \in [0,T].$$

Then a solution to (2), (3), (7) and (8) is unique.

2.3 Inverse Problem 3

For completeness, we consider the inverse problem 3 (IP3) which consists of determining the thermal conductivity $K(t) > 0$, the convection/advection coefficient $Q(t)$ and the temperature $u(x,t)$ satisfying equations (1)–(4), when the heat capacity $C(t)$ is known. By dividing (1) with $C(t)$ we obtain equation (6). Also, dividing (4) by the known $C(t) > 0$ we obtain

$$-a(t)u_x(0,t) = \frac{\nu_1(t)}{C(t)} =: \tilde{\nu}_1(t), \quad a(t)u_x(\ell,t) = \frac{\nu_2(t)}{C(t)} =: \tilde{\nu}_2(t), \quad t \in [0,T]. \tag{9}$$

The following theorems give the unique solvability of solution of the IP3 given by equations (2), (3), (8) and (9).

Theorem 5. (Existence)
Suppose that the following assumptions hold:
(**A1**) $\phi \in C^{2+\gamma}[0,\ell],\ \mu_i \in C^1[0,T],\ \tilde{\nu}_i \in C[0,T]$ *for i=1,2,* $d, f \in C^{\gamma,0}(\Omega)$, *for some* $\gamma \in (0,1)$;
(**A2**) $\phi''(x) > 0,\ x \in [0,\ell],\ \tilde{\nu}_1(t) \geq 0,\ \tilde{\nu}_2(t) \geq 0,\ \tilde{\nu}_2(t) + \tilde{\nu}_1(t) > 0,\ \mu_1'(t) - f(0,t) - d(0,t)\mu_1(t) > 0,\ \mu_2'(t) - f(\ell,t) - d(\ell,t)\mu_2(t) > 0,\ t \in [0,T]$;
(**A3**) $\phi(0) = \mu_1(0),\ \phi(\ell) = \mu_2(0),\ -\tilde{\nu}_1(0)\phi'(\ell) = \tilde{\nu}_2(0)\phi'(0)$.
Then there exists $t_0 \in (0,T]$ *such that the problem (2), (3), (8) and (9) has a (local) solution* $(a(t), b(t), u(x,t)) \in (C[0,t_0])^2 \times C^{2,1}([0,\ell] \times [0,t_0])$ *and* $a(t) > 0, t \in [0,t_0]$.

Proof. Put $x = 0$ and $x = \ell$ into equation (8) and use conditions (3) and (9) to obtain

$$\mu_1'(t) = a(t)u_{xx}(0,t) - \frac{\tilde{\nu}_1(t)b(t)}{a(t)} + d(0,t)\mu_1(t) + f(0,t),$$
$$\mu_2'(t) = a(t)u_{xx}(\ell,t) + \frac{\tilde{\nu}_2(t)b(t)}{a(t)} + d(\ell,t)\mu_2(t) + f(\ell,t).$$

From this we deduce

$$a(t) = \big[(\mu_1'(t) - f(0,t) - d(0,t)\mu_1(t))\tilde{\nu}_2(t) + (\mu_2'(t) - f(\ell,t) - d(\ell,t)\mu_2(t))\tilde{\nu}_1(t)\big] \times (\tilde{\nu}_2(t)u_{xx}(0,t) + \tilde{\nu}_1(t)u_{xx}(\ell,t))^{-1}, \quad t \in [0,T], \tag{10}$$

$$b(t) = a(t)\big[(\mu_2'(t) - f(\ell,t) - d(\ell,t)\mu_2(t))u_{xx}(0,t) - (\mu_1'(t) - f(0,t) - d(0,t)\mu_1(t))u_{xx}(\ell,t)\big] \times (\tilde{\nu}_2(t)u_{xx}(0,t) + \tilde{\nu}_1(t)u_{xx}(\ell,t))^{-1}, \quad t \in [0,T]. \tag{11}$$

To find the solution of the direct problem (2), (3) and (8), we introduce a new unknown function

$$v(x,t) := u(x,t) - \phi(x) - \mu_1(t) + \mu_1(0) - \frac{x}{\ell}(\mu_2(t) - \mu_2(0) - \mu_1(t) + \mu_1(0)). \tag{12}$$

The function $v(x,t)$ satisfies the following problem:

$$v_t = a(t)v_{xx} + b(t)v_x + d(x,t)v + f(x,t) - \mu_1'(t) - \frac{x}{\ell}(\mu_2'(t) - \mu_1'(t)) + a(t)\phi''(x) + b(t)\Big(\phi'(x) + \frac{1}{\ell}(\mu_2(t) - \mu_2(0) - \mu_1(t) + \mu_1(0))\Big) + d(x,t)\Big(\phi(x) + \mu_1(t) - \mu_1(0) + \frac{x}{\ell}(\mu_2(t) - \mu_2(0) - \mu_1(t) + \mu_1(0))\Big), \quad (x,t) \in \Omega, \tag{13}$$

$$v(x,0) = 0, \quad x \in [0,\ell], \tag{14}$$

$$v(0,t) = v(\ell,t) = 0, \quad t \in [0,T]. \tag{15}$$

The solution of problem (12)–(14) is given by the Green's formula and using (12) we obtain

$$u(x,t) = \phi(x) + \mu_1(t) - \mu_1(0) + \frac{x}{\ell}(\mu_2(t) - \mu_2(0) - \mu_1(t) + \mu_1(0))$$
$$+ \int_0^t \int_0^\ell G(x,t;\xi,\tau)\Big[f(\xi,\tau) - \mu_1'(\tau) - \frac{\xi}{\ell}(\mu_2'(\tau) - \mu_1'(\tau)) + a(\tau)\phi''(\xi)$$
$$+ b(\tau)\Big(\phi'(\xi) + \frac{1}{\ell}(\mu_2(\tau) - \mu_2(0) - \mu_1(\tau) + \mu_1(0))\Big)$$
$$+ d(\xi,\tau)\Big(\phi(\xi) + \mu_1(\tau) - \mu_1(0) + \frac{\xi}{\ell}(\mu_2(\tau) - \mu_2(0) - \mu_1(\tau) + \mu_1(0))\Big)\Big] d\xi d\tau, \quad (x,t) \in \overline{\Omega}, \tag{16}$$

where $G = G(x,t;\xi,\tau)$ is the Green function for the equation $V_t = a(t)V_{xx} + b(t)V_x + d(x,t)V$ with Dirichlet boundary conditions.

Differentiating (16) twice with respect to x we obtain

$$u_{xx}(x,t) = \phi''(x) + \int_0^t d\tau \int_0^\ell G_{xx}(x,t;\xi,\tau)\Big[f(\xi,\tau) - \mu_1'(\tau) - \frac{\xi}{\ell}(\mu_2'(\tau) - \mu_1'(\tau)) + a(\tau)\phi''(\xi)$$
$$+ b(\tau)\Big(\phi'(\xi) + \frac{1}{\ell}(\mu_2(\tau) - \mu_2(0) - \mu_1(\tau) + \mu_1(0)\Big) + d(\xi,\tau)\Big(\phi(\xi) + \mu_1(\tau) - \mu_1(0)$$
$$+ \frac{\xi}{\ell}(\mu_2(\tau) - \mu_2(0) - \mu_1(\tau) + \mu_1(0))\Big)\Big] d\xi, \quad (x,t) \in \overline{\Omega}. \tag{17}$$

It is known, [12], that the estimate

$$\left| \int_0^\ell G_{xx}(x,t;\xi,\tau)F(\xi,\tau)d\xi \right| \le \frac{const}{(t-\tau)^{1-\gamma/2}} \tag{18}$$

is true if the function $F(x,t)$ is continuous in $\overline{\Omega}$ and verifies the Hölder condition with respect to x with the exponent γ.

As $\phi''(x) > 0,\ x \in [0,\ell]$, and $\phi \in C^{2+\gamma}[0,\ell]$ we have that there exits $M_0 > 0$ such that $\phi''(x) \ge M_0 > 0,\ x \in [0,\ell]$. Taking into account (18), we conclude that there exists $t_0 \in (0,T]$ such that the estimation

$$\Big| \int_0^t d\tau \int_0^\ell G_{xx}(x,t;\xi,\tau)\Big[f(\xi,\tau) - \mu_1'(\tau) - \frac{\xi}{\ell}(\mu_2'(\tau) - \mu_1'(\tau)) + a(\tau)\phi''(\xi)$$
$$+ b(\tau)\Big(\phi'(\xi) + \frac{1}{\ell}(\mu_2(\tau) - \mu_2(0) - \mu_1(\tau) + \mu_1(0))\Big) + d(\xi,\tau)\Big(\phi(\xi) + \mu_1(\tau) - \mu_1(0)$$
$$+ \frac{\xi}{\ell}(\mu_2(\tau) - \mu_2(0) - \mu_1(\tau) + \mu_1(0))\Big)\Big] d\xi \Big| \le \frac{1}{2}M_0, \quad (x,t) \in [0,\ell] \times [0,t_0] \tag{19}$$

holds. Then

$$u_{xx}(x,t) \ge \frac{1}{2}M_0, \quad (x,t) \in [0,\ell] \times [0,t_0] \tag{20}$$

and the denominator in (10) and (11) may be estimated as follows:

$$\tilde{\nu}_2(t)u_{xx}(0,t) + \tilde{\nu}_1(t)u_{xx}(\ell,t) \geq \frac{1}{2}M_0(\tilde{\nu}_2(t) + \tilde{\nu}_1(t)) \geq M_1 > 0, \quad t \in [0, t_0], \tag{21}$$

for some $M_1 > 0$. Applying this estimate to (10), we obtain

$$a(t) \leq A_1 < \infty, \quad t \in [0, t_0], \tag{22}$$

where the constant A_1 is defined by the input data.

Using the estimation (19) in (17), we obtain that

$$u_{xx}(x,t) \leq \max_{[0,\ell]} \phi''(x) + \frac{1}{2}M_0 =: M_2 < \infty, \quad (x,t) \in [0,\ell] \times [0, t_0]. \tag{23}$$

Taking into account (21)-(23), we deduce from (10) and (11) that

$$a(t) \geq A_0 > 0, \quad |b(t)| \leq B < \infty, \quad t \in [0, t_0], \tag{24}$$

where the constants A_0 and B are defined by the input data.

Now we can apply the Schauder fixed-point theorem to the system of equations (10) and (11). Let us rewrite this system in the form

$$\omega = P\omega,$$

where $\omega := (a(t), b(t))$ and $P := (P_1, P_2)$. Here the operator P_1 is defined by the right-hand side of the equation (10) after substituting into it the expression of u_{xx} from (17), and the operator P_2 is defined by the right-hand side of the equation (11) after substituting into it the expressions of u_{xx} and $a(t)$ from (17) and (10), respectively. It is clear that the operator P maps the set $\mathcal{N} := \{(a, u) : A_0 \leq a(t) \leq A_1, |b(t)| \leq B\}$ into itself. The compactness of the operator P is established by the same way as in [16]. Consequently, there exists at least one fixed point of the operator P in $\mathcal{N}$, that means the existence of solution $(a(t), b(t))$ to the system of equations (10) and (11). After this, the function $u(x,t)$ is determined by (16), and the proof is complete.

Theorem 6. (Uniqueness)
Suppose that the following assumptions hold:

(**A4**) $d \in C^{\gamma,0}(\Omega), for some\ \gamma \in (0,1)$;

(**A5**) $\tilde{\nu}_1(t) \geq 0$, $\tilde{\nu}_2(t) \geq 0$, $\tilde{\nu}_2(t) + \tilde{\nu}_1(t) > 0$, $\mu_1'(t) - f(0,t) - d(0,t)\mu_1(t) > 0$, $\mu_2'(t) - f(\ell,t) - d(\ell,t)\mu_2(t) > 0$, $t \in [0,T]$.

Then the problem (2), (3), (8) and (9) can have at most one solution $(a(t), b(t), u(x,t)) \in (C[0,T])^2 \times C^{2+\gamma,1}(\overline{\Omega})$ *such that* $a(t) > 0, t \in [0,T]$.

Proof. Suppose that the problem (2), (3), (8) and (9) has two different solutions $(a_i(t), b_i(t), u_i(x,t))$, $i \in \{1, 2\}$. Denote $a := a_1 - a_2, b := b_1 - b_2, u := u_1 - u_2$. The triplet of functions $(a(t), b(t), u(x,t))$ is a solution of the following problem:

$$u_t = a_1(t)u_{xx} + b_1(t)u_x + d(x,t)u + a(t)u_{2xx}(x,t) + b(t)u_{2x}(x,t), \quad (x,t) \in \Omega, \tag{25}$$

$$u(x,0) = 0, \quad x \in [0,\ell], \tag{26}$$

$$u(0,t) = 0, \quad u(l,t) = 0, \quad t \in [0,T], \tag{27}$$

$$a_1(t)u_x(0,t) = -a(t)u_{2x}(0,t), \quad a_1(t)u_x(\ell,t) = -a(t)u_{2x}(\ell,t), \quad t \in [0,T]. \tag{28}$$

The solution of the problem (25)-(27) has the following form:

$$u(x,t) = \int_0^t \int_0^\ell G^{(1)}(x,t;\xi,\tau)(a(\tau)u_{2\xi\xi}(\xi,\tau) + b(\tau)u_{2\xi}(\xi,\tau))d\xi d\tau, \quad (x,t) \in \overline{\Omega}, \tag{29}$$

where $G^{(1)}(x,t;\xi,\tau)$ is the Green function for the equation $V_t = a_1(t)V_{xx} + b_1(t)V_x + d(x,t)V$ with Dirichlet boundary conditions. After putting $x = 0$ and $x = \ell$ into equation (25) and using the conditions (28) we obtain the system of equations

$$\begin{cases} \left(u_{2xx}(0,t) + \frac{\tilde{\nu}_1(t)b_1(t)}{a_1(t)a_2(t)}\right)a(t) - \frac{\tilde{\nu}_1(t)}{a_2(t)}b(t) = -a_1(t)u_{xx}(0,t), \quad t \in [0,T], \\ \left(u_{2xx}(\ell,t) - \frac{\tilde{\nu}_2(t)b_1(t)}{a_1(t)a_2(t)}\right)a(t) + \frac{\tilde{\nu}_2(t)}{a_2(t)}b(t) = -a_1(t)u_{xx}(\ell,t), \quad t \in [0,T]. \end{cases}$$

Solving this system we obtain

$$a(t) = -\frac{a_1(t)(\tilde{\nu}_2(t)u_{xx}(0,t) + \tilde{\nu}_1(t)u_{xx}(\ell,t))}{\tilde{\nu}_2(t)u_{2xx}(0,t) + \tilde{\nu}_1(t)u_{2xx}(\ell,t)}, \tag{30}$$

$$b(t) = a_1(t)\Bigg[-u_{2xx}(0,t)u_{xx}(\ell,t) + u_{2xx}(\ell,t)u_{xx}(0,t) - \frac{b_1(t)}{a_1(t)a_2(t)}\Big(\tilde{\nu}_1(t)u_{xx}(\ell,t)$$
$$+ \tilde{\nu}_2(t)u_{xx}(0,t)\Big)\Bigg](\tilde{\nu}_2(t)u_{2xx}(0,t) + \tilde{\nu}_1(t)u_{2xx}(\ell,t))^{-1}, \quad t \in [0,T]. \tag{31}$$

Let us verify that

$$\tilde{\nu}_2(t)u_{2xx}(0,t) + \tilde{\nu}_1(t)u_{2xx}(\ell,t) \neq 0, \quad t \in [0,T]. \tag{32}$$

As $(a_2(t), b_2(t), u_2(x,t))$ is a solution to the problem (2), (3), (8) and (9) we have from (10) that

$$a_2(t) = \big[(\mu_1'(t) - f(0,t) - d(0,t)\mu_1(t))\tilde{\nu}_2(t) + (\mu_2'(t) - f(\ell,t) - d(\ell,t)\mu_2(t))\tilde{\nu}_1(t)\big]$$
$$\times (\tilde{\nu}_2(t)u_{2xx}(0,t) + \tilde{\nu}_1(t)u_{2xx}(\ell,t))^{-1}, \quad t \in [0,T].$$

Here $a_2(t) > 0, t \in [0,T]$ and $(\mu_1'(t) - f(0,t) - d(0,t)\mu_1(t))\tilde{\nu}_2(t) + (\mu_2'(t) - f(\ell,t) - d(\ell,t)\mu_2(t))\tilde{\nu}_1(t) > 0$, as a consequence of the assumption **(A5)**. Hence, the inequality (32) is true. It means that we have a system of homogeneous Volterra integral equations (30) and (31) whose kernels verify the estimate (18). It yields that $a(t) \equiv 0, b(t) \equiv 0, t \in [0,T]$. Then, from (29) we also obtain that $u(x,t) \equiv 0, (x,t) \in \overline{\Omega}$, and the proof is complete.

3 Solution of Direct Problem

In this section, we consider the direct initial boundary value problem given by equations (2), (3) and (8), where $a(t)$, $b(t)$, $d(x,t)$, $f(x,t)$, $\phi(x)$ and $\mu_i(t)$, $i = 1, 2$, are known and the solution $u(x,t)$ is to be determined. To achieve this, we use the Crank-Nicolson finite-difference scheme [29], which is unconditionally stable and second-order accurate in space and time.

The discrete form of our problem is as follows. We divide the domain $\Omega = (0, \ell) \times (0, T)$ into M and N subintervals of equal step length h and k, where $h = \frac{\ell}{M}$ and $k = \frac{T}{N}$, respectively. So, the solution at the node (i, j) is $u_{i,j} := u(x_i, t_j)$, where $x_i = ih$, $t_j = jk$, for $i = \overline{0, M}$, $j = \overline{0, N}$.

Considering the general partial differential equation

$$u_t = F(x, t, u, u_x, u_{xx}), \tag{33}$$

the Crank-Nicolson method is based on central finite-difference approximations for space and forward finite-difference approximations for time which gives second-order convergence rate. This method is equivalent to take average of forward and backward Euler schemes in time, hence equation (33) can approximated as:

$$\frac{u_{i,j+1} - u_{i,j}}{k} = \frac{1}{2}\left(F_{i,j} + F_{i,j+1}\right), \qquad i = \overline{1, (M-1)}, j = \overline{0, (N-1)}, \tag{34}$$

$$u_{i,0} = \phi(x_i), \qquad i = \overline{0, M}, \tag{35}$$

$$u_{0,j} = \mu_1(t_j), \qquad j = \overline{0, N}, \tag{36}$$

$$u_{M,j} = \mu_2(t_j), \qquad j = \overline{0, N}. \tag{37}$$

For our problem, equation (8) can be discretised in the form of (34) as

$$\begin{aligned} &- A_{j+1}u_{i-1,j+1} + (1 - B_{i,j+1})u_{i,j+1} - C_{j+1}u_{i+1,j+1} = \\ &\qquad - A_j u_{i-1,j} + (1 + B_{i,j})u_{i,j} - C_j u_{i+1,j} + \frac{k}{2}\left(f_{i,j+1} + f_{i,j}\right) \end{aligned} \tag{38}$$

for $i = \overline{1, (M-1)}$, $j = \overline{0, N}$, where $f_{i,j} := f(x_i, t_j)$

$$A_j = \frac{k}{2h^2}a(t_j) - \frac{k}{4h}b(t_j), \quad B_{i,j} = -\frac{k}{h^2}a(t_j) + \frac{k}{2}d(x_i, t_j), \quad C_j = \frac{k}{2h^2}a(t_j) + \frac{k}{4h}b(t_j).$$

At each time step t_{j+1}, for $j = \overline{0, (N-1)}$, using the Dirichlet boundary conditions (3), the above difference equation can be reformulated as a $(M-1) \times (M-1)$ linear system of equations of the form,

$$L\mathbf{u} = \mathbf{b}$$

where

$$\mathbf{u} = (u_{1,j+1}, u_{2,j}, ..., u_{M-1,j+1})^{tr}, \quad \mathbf{b} = (b_1, b_2, ..., b_{M-1})^{tr}.$$

and

$$L = \begin{pmatrix} 1 - B_{0,j+1} & -(A_{j+1} + C_{j+1}) & 0 & \cdots & 0 & 0 & 0 \\ -A_{j+1} & 1 - B_{1,j+1} & -C_{j+1} & \cdots & 0 & 0 & 0 \\ \vdots & \vdots & \vdots & \ddots & \vdots & \vdots & \vdots \\ 0 & 0 & 0 & \cdots & -A_{j+1} & 1 - B_{M-2,j+1} & -C_{j+1} \\ 0 & 0 & 0 & \cdots & 0 & -(A_{j+1} + C_{j+1}) & 1 - B_{M-1,j+1} \end{pmatrix}$$

$$b_1 = (1 + B_{0,j})u_{0,j} + (A_j + C_j)u_{1,j} - 2h(C_{j+1}\mu_1(t_{j+1}) + C_j\mu_1(t_j)) + \frac{k}{2}(f_{0,j+1} + f_{0,j}),$$

$$b_i = A_j u_{i-1,j} + (1 + B_{i,j})u_{i,j} + C_j u_{i+1,j} + \frac{k}{2}(f_{i,j+1} + f_{i,j}), \qquad i = \overline{2, (M-2)},$$

$$\begin{aligned} b_{M-1} = &(A_j + C_j)u_{M-2,j} + (1 + B_{M-1,j})u_{0,j} + 2h(A_{j+1}\mu_2(t_{j+1}) + A_j\mu_2(t_j)) \\ &+ \frac{k}{2}(f_{M-1,j+1} + f_{M-1,j}). \end{aligned}$$

As an example, consider the direct problem (2), (3) and (8) with $T = \ell = 1$ and

$$a(t) = 1 + t, \quad b(t) = 1 + 2t, \quad d(x,t) = x^2 + t^2, \quad \phi(x) = (1-3x)^2, \quad \mu_1(t) = e^t,$$
$$\mu_2(t) = 4e^t, \; f(x,t) = (1-3x)^2 e^t - 18(1+t)e^t + (6+12t)(1-3x)e^t$$
$$- (x^2+t^2)(1-3x)^2 e^t.$$

With this input data, the exact solution is given by $u(x,t) = (1-3x)^2 e^t$, and the desired heat fluxes (4), for $K(t) = 1$, are $\nu_1(t) = 6e^t$ and $\nu_2(t) = 12e^t$.

The numerical and exact solutions for $u(x,t)$ are shown in Figure 1 and very good agreement is obtained. Tables 1 and 2 give the numerical heat fluxes in comparison with the exact ones. These have been calculated using the following $O(h^2)$ finite-difference approximations:

$$u_x(0,t_j) = \frac{4u_{1,j} - u_{2,j} - 3u_{0,j}}{2h}, \; u_x(\ell,t_j) = \frac{4u_{M-1,j} - u_{M-2,j} - 3u_{M,j}}{-2h}, \; j = \overline{1,N}. \quad (39)$$

From these tables it can be seen that the numerical results are in very good agreement with the exact solution and that a rapid monotonic increasing convergence is achieved.

Table 1: The exact and the numerical heat flux $-u_x(0,t)$ for $M = N \in \{10, 20, 40, 100\}$, for the direct problem.

t	0.1	0.2	...	0.8	0.9	1
$M = N = 10$	-6.6309	-7.3282	...	-13.3529	-14.7573	-16.3093
$M = N = 20$	-6.6310	-7.3284	...	-13.3532	-14.7575	-16.3096
$M = N = 40$	-6.6310	-7.3284	...	-13.3532	-14.7576	-16.3097
$M = N = 100$	-6.6310	-7.3284	...	-13.3532	-14.7576	-16.3097
exact	-6.6310	-7.3284	...	-13.3532	-14.7576	-16.3097

Table 2: The exact and the numerical heat flux $u_x(1,t)$ for $M = N \in \{10, 20, 40, 100\}$, for the direct problem.

t	0.1	0.2	...	0.8	0.9	1
$M = N = 10$	13.2614	14.6564	...	26.7059	29.5145	23.6187
$M = N = 20$	13.2620	14.6567	...	26.7063	29.5151	23.6192
$M = N = 40$	13.2620	14.6568	...	26.7064	29.5152	23.6193
$M = N = 100$	13.2620	14.6568	...	26.7056	29.5152	23.6194
exact	13.2620	14.6568	...	26.7065	29.5152	23.6194

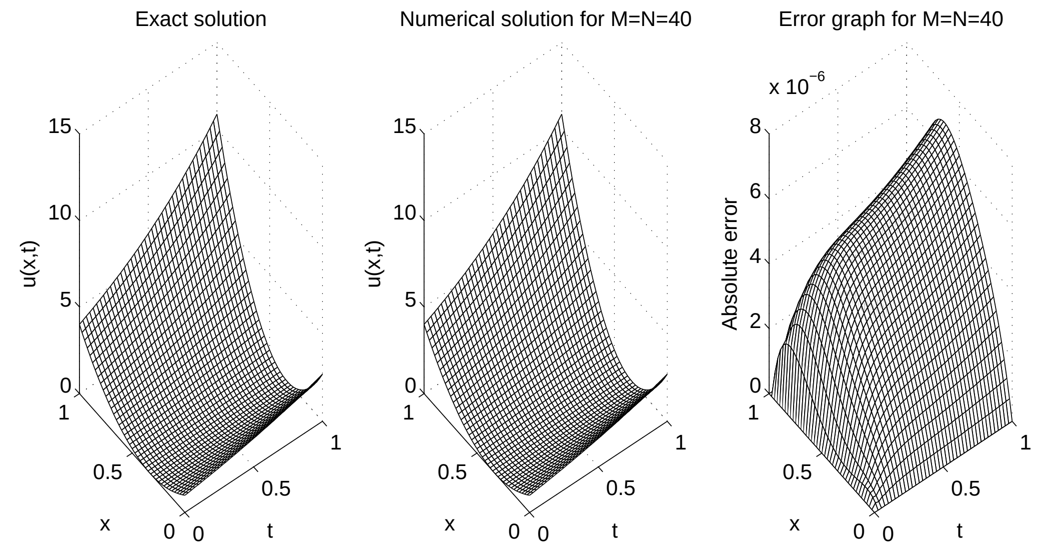

Figure 1: Exact and numerical solutions for $u(x,t)$ and the absolute error for the direct problem (2), (3) and (8) obtained with $M = N = 40$.

4 Solution of Inverse Problems

In our inverse problems we wish to obtain simultaneously stable reconstructions of two unknown coefficients in equation (1), satisfying the initial and boundary conditions (2)–(4). The most common Tikhonov-type regularization approach is to impose the measured input data (4) in a penalised least-squares sense. This recasts into minimizing the following regularised (penalised) nonlinear objective functions.

For the IP1 given by equations (2)–(5) we minimize the functional

$$F_1(K,a) := \| -K(t)u_x(0,t) - \nu_1(t)\|^2 + \|K(t)u_x(\ell,t) - \nu_2(t)\|^2 \\ + \beta\left(\|K(t)\|^2 + \|a(t)\|^2\right), \tag{40}$$

where $\beta \geq 0$ is a regularization parameter and the norm $\|\cdot\|$ is usually taken as the $L^2[0,T]$ norm.

For the IP2 given by equations (2), (3), (7) and (8) we minimize the functional

$$F_2(a,b) := \| -u_x(0,t) - \overline{\nu}_1(t)\|^2 + \|u_x(\ell,t) - \overline{\nu}_2(t)\|^2 \\ + \beta\left(\|a(t)\|^2 + \|b(t)\|^2\right). \tag{41}$$

For the IP3 given by equations (2)–(4) and (8) we minimize the functional

$$F_3(K,b) := \| -K(t)u_x(0,t) - \nu_1(t)\|^2 + \|K(t)u_x(\ell,t) - \nu_2(t)\|^2 \\ + \beta\left(\|K(t)\|^2 + \|b(t)\|^2\right). \tag{42}$$

The case $\beta = 0$ yields the ordinary nonlinear least-squares method which is usually unstable. The physical constraints that the thermal conductivity and diffusivity are positive recast as a simple lower bound on these variable and is imposed as $K \geq 10^{-10}$ and $a \geq 10^{-10}$. The velocity v of the fluid is allowed to be either positive (convection) or negative (advection).

The discretisations of (40)–(42) are:

$$F_1(\underline{K},\underline{a}) = \sum_{j=0}^{N}[-K(t_j)u_x(0,t_j) - \nu_1(t_j)]^2 + \sum_{j=0}^{N}[K(t_j)u_x(\ell,t_j) - \nu_2(t_j)]^2 + \beta\left(\sum_{j=0}^{N}K^2(t_j) + \sum_{j=0}^{N}a^2(t_j)\right), \tag{43}$$

$$F_2(\underline{a},\underline{b}) = \sum_{j=0}^{N}[-u_x(0,t_j) - \overline{\nu}_1(t_j)]^2 + \sum_{j=0}^{N}[u_x(\ell,t_j) - \overline{\nu}_2(t_j)]^2 + \beta\left(\sum_{j=0}^{N}a^2(t_j) + \sum_{j=0}^{N}b^2(t_j)\right), \tag{44}$$

$$F_3(\underline{K},\underline{b}) = \sum_{j=0}^{N}[-K(t_j)u_x(0,t_j) - \nu_1(t_j)]^2 + \sum_{j=0}^{N}[K(t_j)u_x(\ell,t_j) - \nu_2(t_j)]^2 + \beta\left(\sum_{j=0}^{N}K^2(t_j) + \sum_{j=0}^{N}b^2(t_j)\right), \tag{45}$$

respectively.

It is worth mentioning that at the first time step, i.e. $j = 0$, the above equations (43)–(45) need to calculate the derivatives $u_x(0,0)$ and $u_x(\ell,0)$ which are obtained from the initial condition (2), using (39) as:

$$u_x(0,0) = \frac{4\phi_1 - \phi_2 - 3\phi_0}{2h}, \quad u_x(\ell,0) = \frac{4\phi_{M-1} - \phi_{M-2} - 3\phi_M}{-2h}, \tag{46}$$

where $\phi_i = \phi(x_i)$ for $i = \overline{0,M}$.

If there is noise in the measured data (4), we replace $\nu_1(t_j)$ and $\nu_2(t_j)$ in (43) and (45) by the noisy perturbations

$$\nu_1^{\epsilon 1}(t_j) = \nu_1(t_j) + \epsilon 1_j, \quad \nu_2^{\epsilon 2}(t_j) = \nu_2(t_j) + \epsilon 2_j, \quad j = \overline{0,N}, \tag{47}$$

where $\epsilon 1_j$ and $\epsilon 2_j$ are random variables generated from a Gaussian normal distribution with mean zero and standard deviations σ_1 and σ_2, respectively, given by

$$\sigma_1 = p \times \max_{t\in[0,T]} |\nu_1(t)|, \quad \sigma_2 = p \times \max_{t\in[0,T]} |\nu_2(t)|, \tag{48}$$

where p represents the percentage of noise. We use the MATLAB function *normrnd* to generate the random variables $\underline{\epsilon 1}$ and $\underline{\epsilon 2}$ as follows:

$$\underline{\epsilon 1} = normrnd(0,\sigma_1,N+1), \quad \underline{\epsilon 2} = normrnd(0,\sigma_2,N+1). \tag{49}$$

Note that via (7) we replace $\overline{\nu_1}$ and $\overline{\nu_2}$ in (44) by the noisy perturbations

$$\overline{\nu}_1^{\epsilon 1}(t_j) = \nu_1^{\epsilon 1}(t_j)/K(t_j), \quad \overline{\nu}_2^{\epsilon 2}(t_j) = \nu_2^{\epsilon 2}(t_j)/K(t_j), \quad j = \overline{0,N}. \tag{50}$$

4.1 Minimization Algorithms

Nevertheless, finding a global minimizer (even only approximately) to nonlinear (least-squares) problems is not an easy task. Numerical experience shows that the objective function which is, in general, non-convex has usually multiple local minima in which a descent method tends to get stuck if the underlying problem is ill-posed. Furthermore, the determination of an appropriate regularization parameter β requires additional computational effort.

In this section, we give brief description of the routines *fmincon* and *lsqnonlin* from the MATLAB Optimization Toolbox [25, 26] that we have employed for the constrained nonlinear minimization of the functionals defined by equations (40)–(42). These routines are based on interior trust region methods for nonlinear minimization, [3, 6].

The above routines attempt to find a minimum of a scalar objective function of several variables, starting from a initial guess, subject to simple bounds on the variables. In all examples of the next section, the initial guess was $K^0 = 1$, $a^0 = 1$, $b^0 = 1$ and the lower and upper bounds were taken as $LB(K) = LB(a) = 10^{-10}$, $LB(b) = -10^3$, and $UB(K) = UB(a) = UB(b) = 10^3$.

Apart from the initial guess, and the upper and lower bounds the routines also require the user to input some parameters such as:

- Number of variables $M = N = 40$.
- Maximum number of iterations $= (10^2 \div 10^5) \times$ (number of variables).
- Maximum number of objective function evaluations $= (10^3 \div 10^7)\times$(number of variables).
- x Tolerance (xTol) $= 10^{-10}$.
- Function Tolerance (FunTol) $= 10^{-10}$.
- Nonlinear constraint tolerance $= 10^{-6}$.

It is also worth noting that the user does not need to supply the gradient of the objective function which is minimized, as this is calculated internally within the routines using finite differences. Further, the Broyden, Fletcher, Goldfarb and Shanno (BFGS) technique is used to compute the Hessian matrix.

We finally mention that we have also used a combination between a generalized pattern search algorithm for the poll method and a genetic algorithm for the search method, both of them from the MATLAB Global Optimization Toolbox. In comparison with the previously described interior-point algorithms the results were not significantly improved, but instead the computational time increased beyond purpose. For this reason, the numerical results obtained using this latter combined method are omitted.

5 Numerical Results and Discussion

Numerical results are presented for several test examples for the inverse problems IP1–IP3, and in each example we obtain the numerical solution of coefficient identification problems for various noise levels p. In these examples we take, for simplicity, $\ell = T = 1$.

We employ $fmincon$ for IP1 and $lsqnonlin$ for IP2 and IP3, for the minimization of the functionals (40)–(42). The other computational details have already been given in Subsection 4.1. We have also calculated the relative root mean square error ($rrmse$) to analyse the error between the exact and estimated coefficients, defined as,

$$rrmse(K(t)) = \sqrt{\frac{1}{N+1}\sum_{j=0}^{N}\left(\frac{K_{numerical}(t_j) - K_{exact}(t_j)}{K_{exact}(t_j)}\right)^2}, \tag{51}$$

and similar expressions exist for $a(t)$, $b(t)$ and $C(t)$.

One of the main difficulty when we solve inverse and ill-posed problems is how to choose an appropriate regularization parameter β which must compromise between accuracy and stability. Nevertheless, one can use techniques such as the L-curve method [13] or, Morozov's discrepancy principle [22] to find such a parameter, but in our work we have used trial and error. As mentioned in [8], the regularization parameter β is selected based on experience by first choosing a small value and gradually increasing it until any numerical oscillations in the unknown coefficient are removed.

5.1 Example 1 for IP1

We first consider the problem IP1 given by equations (2)–(5), with unknown coefficients $C(t)$ and $K(t)$, and we solve this inverse problem with the following input data:

$$\phi(x) = (1+x)^2, \ \mu_1(t) = t^2+t+1, \quad \mu_2(t) = t^2+t+4,$$
$$\nu_1(t) = -(1+t)(1+2t), \quad \nu_2(t) = 2(1+t)(1+2t),$$

for $x \in (0, \ell = 1)$ and $t \in (0, T = 1)$. The exact solution is given by

$$u(x,t) = (1+x)^2 + t^2 + t, \ C(t) = 1+t, \quad K(t) = (1+t)\left(t+\frac{1}{2}\right). \tag{52}$$

We also have that $a(t) = t + \frac{1}{2}$, and one can easily check that the conditions of Theorems 1 and 2 are satisfied such that we know beforehand for sure that the solution to the IP1 exits and is unique.

Table 3 gives the numerical coefficients obtained using $M = N \in \{10, 20, 40\}$ in comparison with the exact ones. Form this table it can be seen that the numerical results are convergent to the exact values, as the FDM mesh size decreases. In the remaining of this section, the FDM discretization with $M = N = 40$ is fixed in order to keep the accuracy good with reasonable computational effort.

Table 3: The exact and the numerical coefficients for $M = N \in \{10, 20, 40\}$, for the IP1 of Example 1 and without noise.

t	0.1	0.2	...	0.8	0.9	1	
	0.6600	0.8400	...	2.3400	2.6600	3.0000	$M = N = 10$
$k(t)$	0.6600	0.8400	...	2.3400	2.6600	3.0000	$M = N = 20$
	0.6600	0.8400	...	2.3400	2.6600	3.0000	$M = N = 40$
	0.6600	0.8400	...	2.3400	2.6600	3.0000	exact
	0.5769	0.7231	...	1.3231	1.3769	1.5231	$M = N = 10$
$a(t)$	0.6183	0.7183	...	1.3183	1.4183	1.5183	$M = N = 20$
	0.6119	0.7119	...	1.3119	1.4119	1.5119	$M = N = 40$
	0.6000	0.7000	...	1.3000	1.4000	1.5000	exact
	1.1441	1.1616	...	1.7686	1.9319	1.9696	$M = N = 10$
$C(t)$	1.0674	1.1694	...	1.7750	1.8755	1.9759	$M = N = 20$
	1.0787	1.1800	...	1.7837	1.8840	1.9843	$M = N = 40$
	1.1000	1.2000	...	1.8000	1.9000	2.0000	exact

In Figure 2, we present the regularized objective function (40) for $p = 0$ (no noise) and $p = 1\%$ noise included in input data $\nu_1(t)$ and $\nu_2(t)$ for several regularization parameters $\beta \in \{0, 10^{-3}, 10^{-2}, 10^{-1}\}$. From this figure it can be seen that convergence is achieved in a relatively small number of iterations. Also, it takes a slightly larger number of iterations when $p = 1\%$ noise contaminates the input data than when this data is errorless, i.e. $p = 0$.

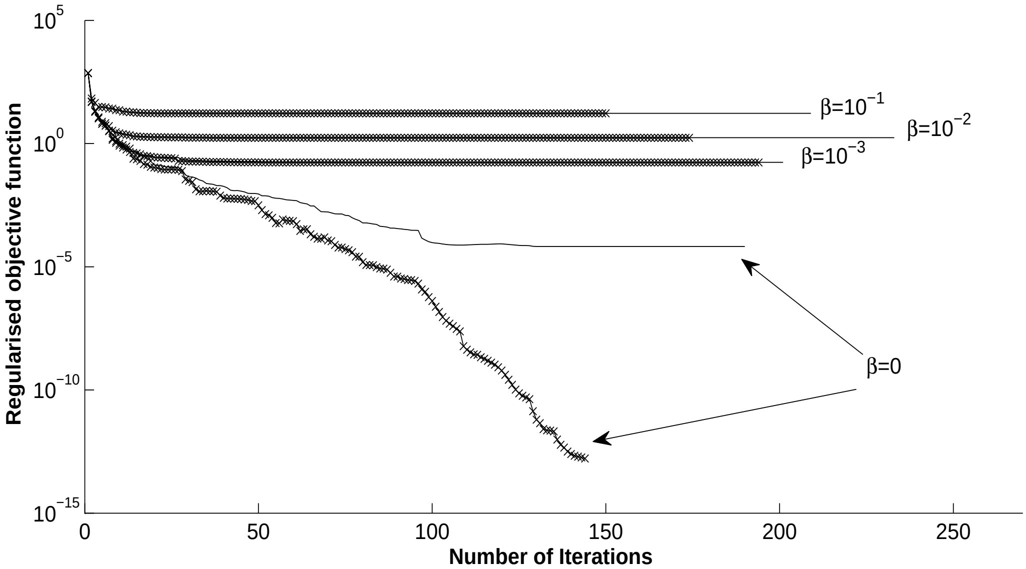

Figure 2: Regularised objective function (40), for Example 1 without noise (-×-) and with $p = 1\%$ noise (—).

In Figure 3 and Table 4, we present the identified coefficients and their $rrmse$ values, respectively, for no noise, and with and without regularization. From this figure and table it can be seen that for exact data, when β decreases to zero we obtain numerical results for the identified coefficients $K(t)$, $a(t)$ and $C(t)$ which are convergent to their exact values. In the case $\beta = 10^{-1}$ we observe that the graphs of the identified coefficients slightly depart from the exact ones because we have added too much unwanted regularization to the objective function (40). In Figure 4 and Table 4 we present the retrieved coefficients and their *rrmse* values, respectively, when $p = 1\%$ noise is included in the input data $\nu_1(t)$ and $\nu_2(t)$. It can be seen that the numerical retrieval of the thermal conductivity $K(t)$ is accurate; however, unstable results are obtained for $a(t)$ and $C(t)$ if no regularization, i.e. $\beta = 0$, is employed, or even if β is too small such as 10^{-3}. Clearly, one can observe the effect of the regularization parameter $\beta > 0$ in decreasing the oscillatory unstable behaviour of the retrieved coefficients. Overall, the numerical results obtained with $\beta = 10^{-1}$ seem the most stable and accurate.

Table 4: The *rrmse* values for estimated coefficients in Example 1.

	$\beta = 0$	$\beta = 10^{-3}$	$\beta = 10^{-2}$	$\beta = 10^{-1}$
	$rrmse(K) = 8.5E-9$	$8.5E-5$	$8.3E-4$	0.0079
$p = 0$	$rrmse(a) = 0.0138$	0.0284	0.0352	0.0781
	$rrmse(C) = 0.0138$	0.0287	0.0385	0.1241
	$rrmse(K) = 0.0142$	0.0143	0.0146	0.0172
$p = 1\%$	$rrmse(a) = 0.2937$	0.2941	0.1654	0.0917
	$rrmse(C) = 0.4059$	0.6279	0.2080	0.1194

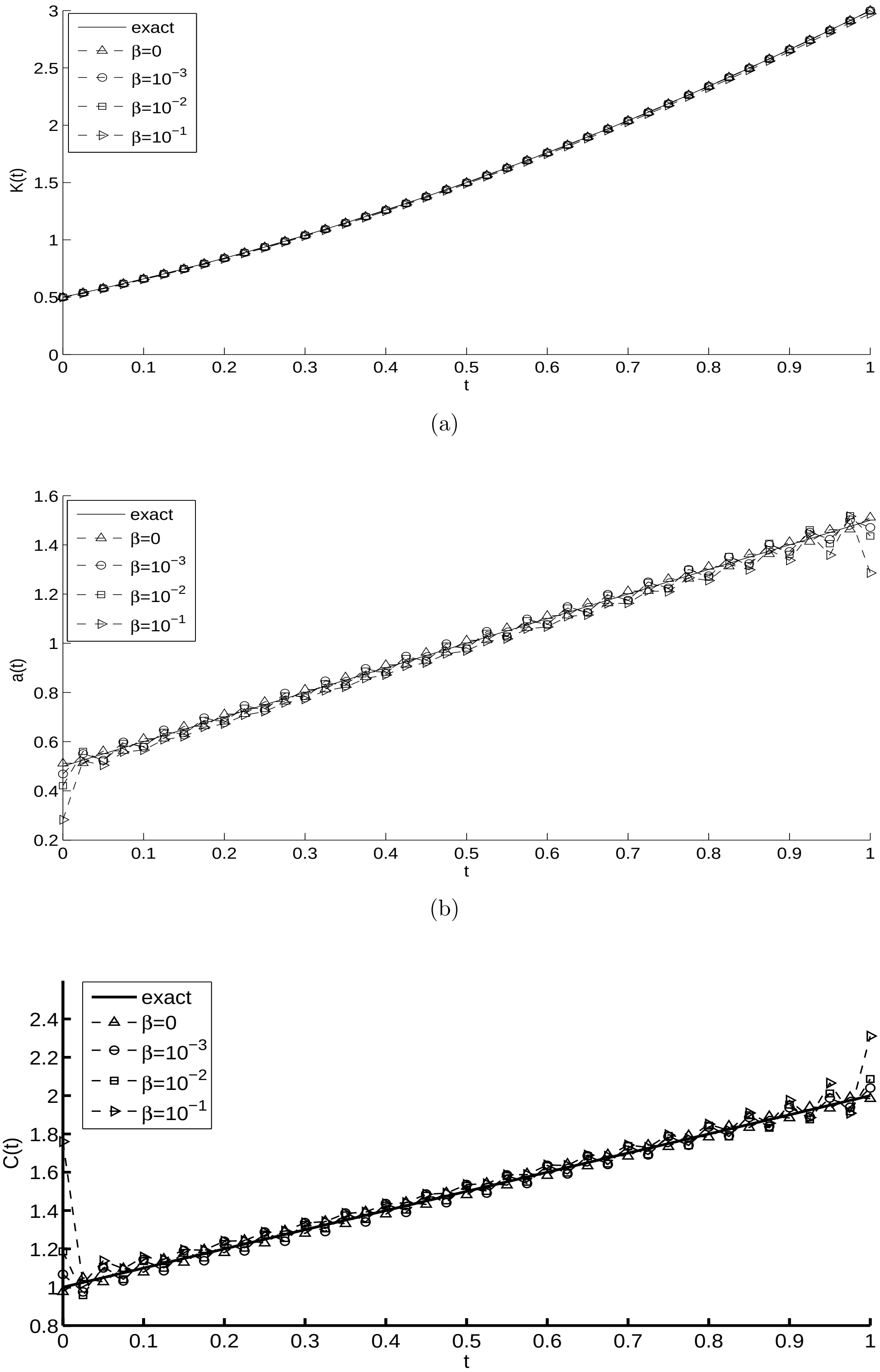

(a)

(b)

(c)

Figure 3: The identified coefficients: (a) Thermal conductivity, (b) Thermal diffusivity, and (c) Heat capacity, for Example 1 with no noise.

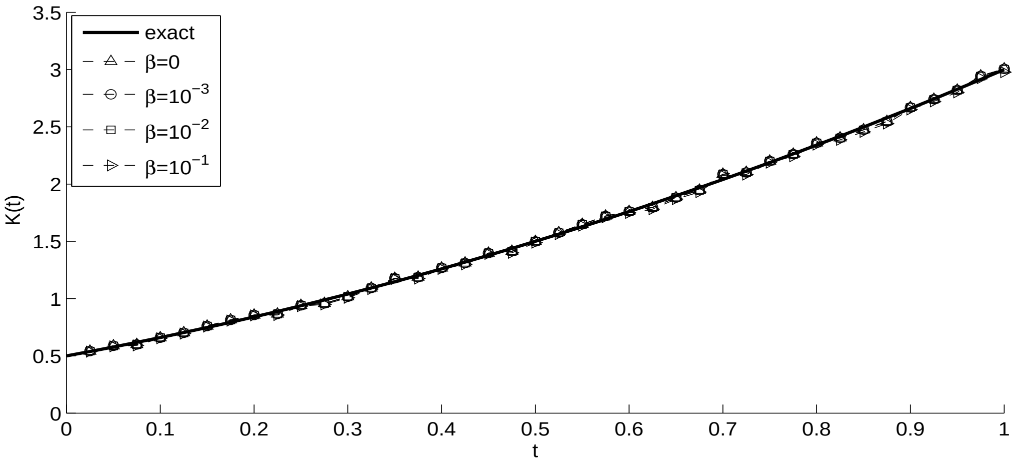

(a)

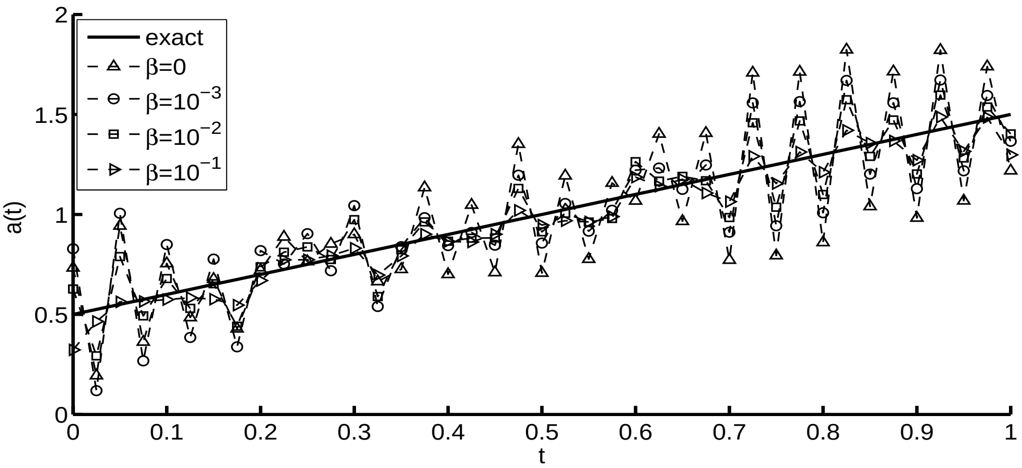

(b)

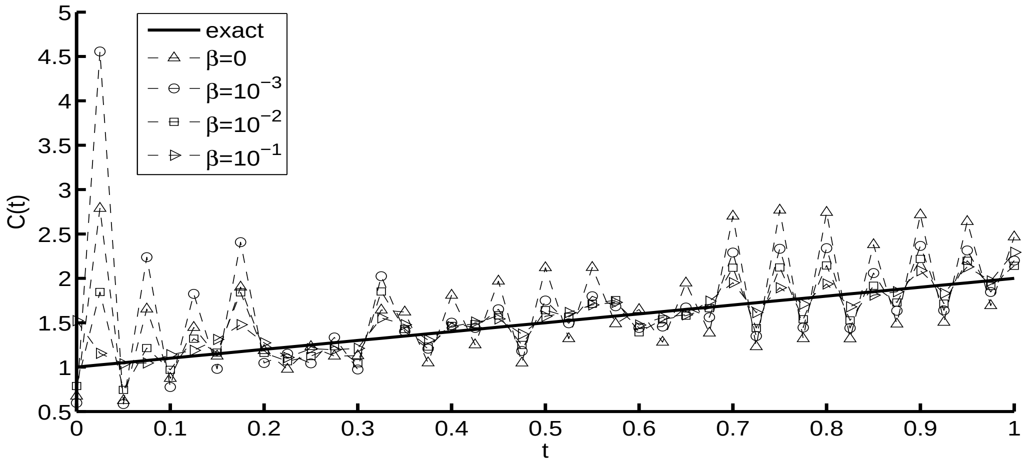

(c)

Figure 4: The identified coefficients: (a) Thermal conductivity, (b) Thermal diffusivity, and (c) Heat capacity, for Example 1 with $p = 1\%$ noise.

5.2 Example 2 for IP1

We next consider an example from [15] in which the input data satisfy the conditions of existence of solution of Theorem 1,

$$\phi(x) = \frac{x^4}{12} + 2x - 4,\ \mu_1(t) = t^4 + 2t^3 + t^2 - 4, \quad \mu_2(t) = t^4 + 2t^3 + 2t^2 + t - \frac{23}{12},$$
$$\nu_1(t) = -2t - 2, \qquad \nu_2(t) = (t+1)\left(2t^2 + 2t + \frac{7}{3}\right),$$

for $x \in (0, \ell = 1)$ and $t \in (0, T = 1)$. However, the conditions of uniqueness of solution of Theorem 2 are all satisfied, but for the condition $\phi''(0) > 0$ which is not satisfied. One can simply check by direct substitution that the solution

$$u(x,t) = t^4 + 2t^3 + t^2(x^2+1) + tx^2 + \frac{x^4}{12} + 2x - 4,$$
$$C(t) = \frac{1+t}{1+2t}, \quad K(t) = 1 + t. \tag{53}$$

satisfies the inverse problem (2)–(5). We also have that $a(t) = 1 + 2t$.

Figure 5 illustrates the objective function (40), as a function of the number of iterations for $p = 0$ (no noise) and $p = 1\%$ noise included in the input data $\nu_1(t)$ and $\nu_2(t)$. It is interesting to remark that for β small such as 0 to 10^{-3} the convergence is non-monotonic with respect to the number of iterations. Also, the unregularized ($\beta = 0$) objective function reduces rather non-smoothly to reach a stationary value of $O(10^{-7})$ for $p = 0$ and $O(10^{-4})$ for $p = 1\%$, whilst the curves obtained for $\beta > 0$ reach rapidly a stationary plateau.

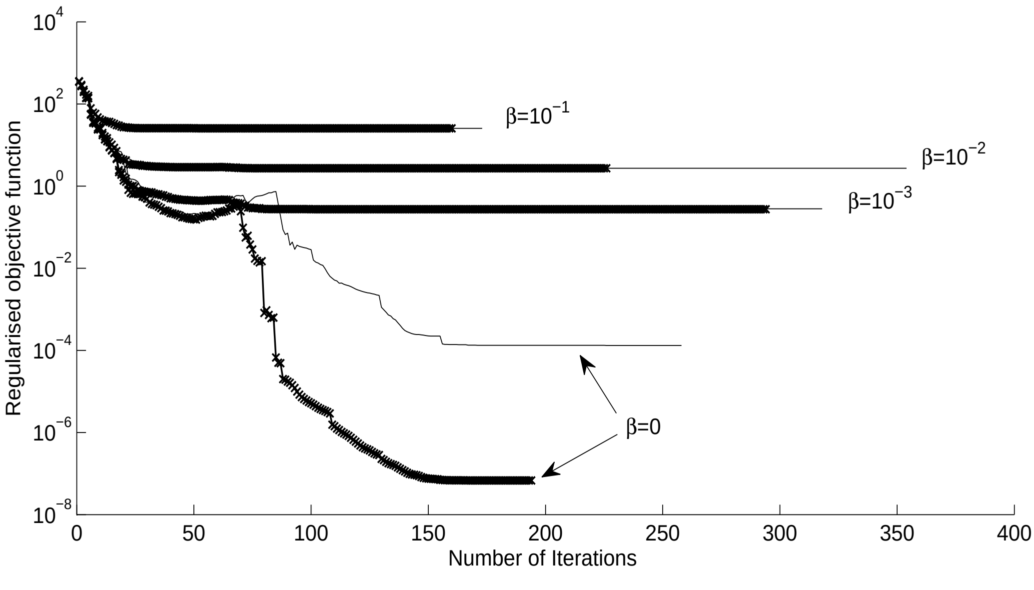

Figure 5: Regularised objective function (40), for Example 2 without noise (-×-) and with $p = 1\%$ noise (—).

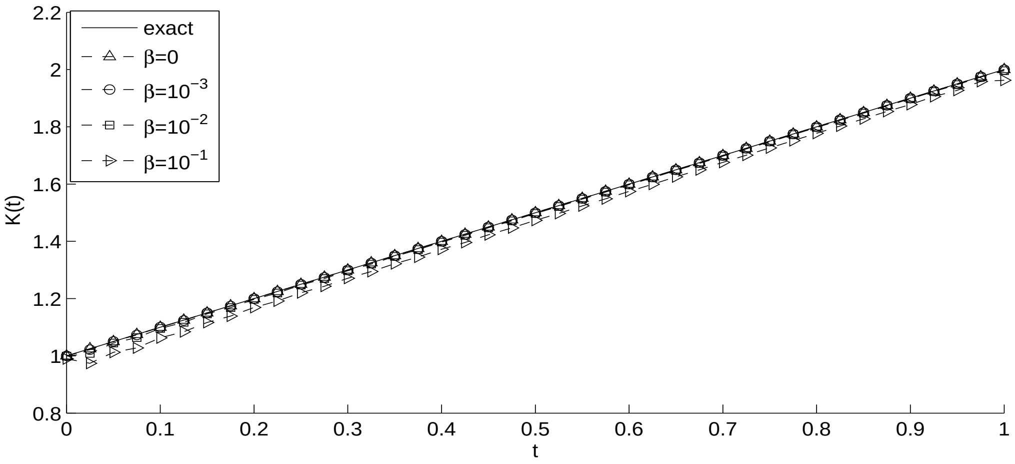

(a)

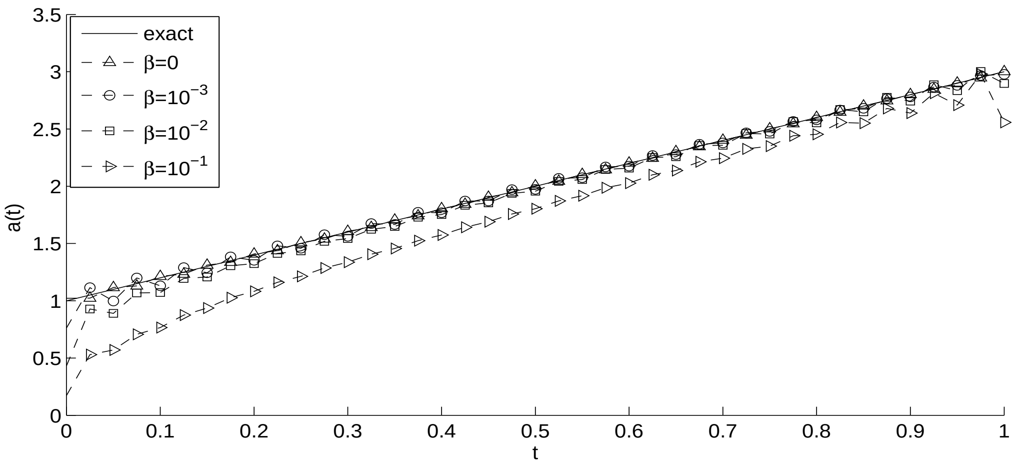

(b)

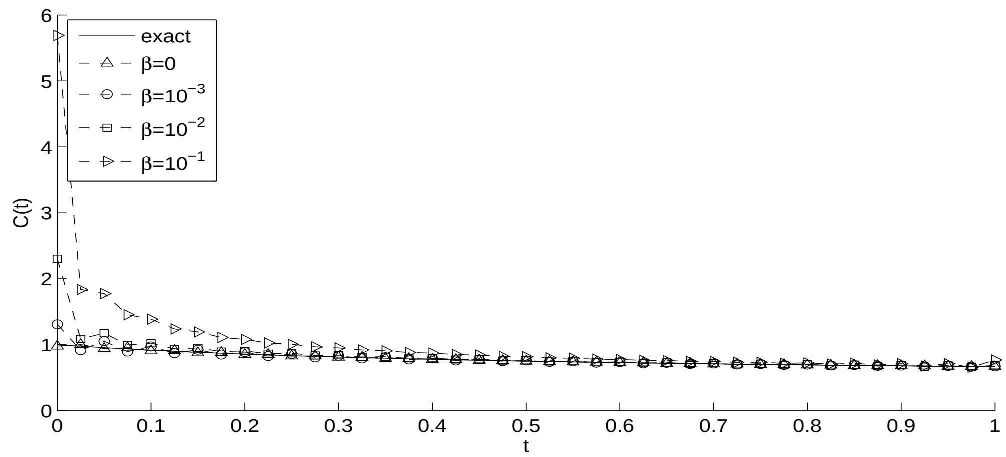

(c)

Figure 6: The identified coefficients: (a) Thermal conductivity, (b) Thermal diffusivity, and (c) Heat capacity, for Example 2 with no noise.

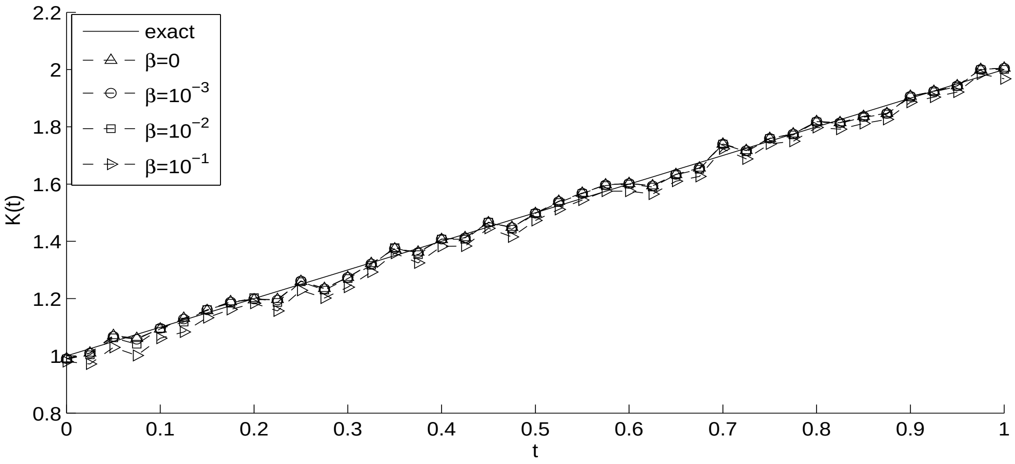

(a)

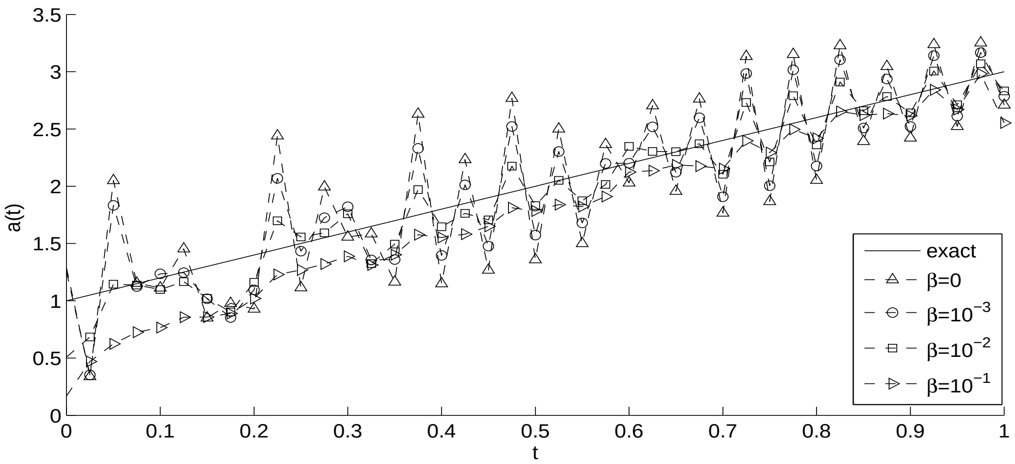

(b)

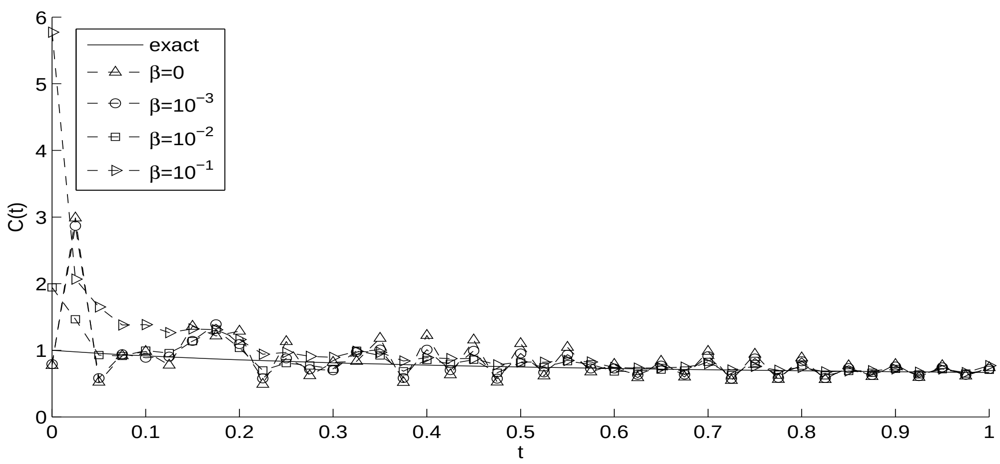

(c)

Figure 7: The identified coefficients: (a) Thermal conductivity, (b) Thermal diffusivity, and (c) Heat capacity, for Example 2 with $p = 1\%$ noise.

Figures 6, 7 and Table 5 for Example 2 represent the same quantities as Figures 3, 4 and Table 4 for Example 1, and the same conclusions can be drawn. We also mention that the numerical results obtained with $\beta = 10^{-2}$ seem the most stable and accurate for $p = 1\%$ noisy data.

Table 5: The $rrmse$ values for estimated coefficients in Example 2.

	$\beta = 0$	$\beta = 10^{-3}$	$\beta = 10^{-2}$	$\beta = 10^{-1}$
$p = 0$	$rrmse(K) = 5.6E-5$	$6.8E-4$	0.0039	0.0223
	$rrmse(a) = 0.0078$	0.0449	0.1000	0.2239
	$rrmse(C) = 0.0078$	0.0552	0.2095	0.7778
$p = 1\%$	$rrmse(K) = 0.0123$	0.0125	0.0146	0.0276
	$rrmse(a) = 0.3066$	0.2301	0.1441	0.2321
	$rrmse(C) = 0.4350$	0.3677	0.2135	0.7993

5.3 Example 3 for IP1

Finally, for IP1, we consider the case of a non-smooth coefficient and more complicated input data given by

$$\phi(x) = \frac{x^2 + x}{2} - \frac{1}{4},$$
$$\mu_1(t) = \begin{cases} \frac{3t-t^2}{2} - \frac{1}{4} & \text{if } t \in [0, \frac{1}{2}] \\ \frac{t+t^2}{2} & \text{if } t \in [\frac{1}{2}, 1] \end{cases}, \quad \mu_2(t) = \begin{cases} \frac{3t-t^2}{2} + \frac{3}{4} & \text{if } t \in [0, \frac{1}{2}] \\ \frac{t+t^2}{2} + 1 & \text{if } t \in [\frac{1}{2}, 1] \end{cases},$$
$$\nu_1(t) = -\frac{1}{2}\left(1 + \left|t - \frac{1}{2}\right|\right), \qquad \nu_2(t) = \frac{3}{2}\left(1 + \left|t - \frac{1}{2}\right|\right),$$

for $x \in (0, \ell = 1)$ and $t \in (0, T = 1)$. One can remark that the conditions of Theorem 2 which ensure the uniqueness of solution are satisfied. The exact solution is given by

$$u(x,t) = \frac{x + x^2}{2} + \begin{cases} \frac{3t-t^2}{2} - \frac{1}{4} & \text{if } t \in [0, \frac{1}{2}] \\ \frac{t+t^2}{2} & \text{if } t \in [\frac{1}{2}, 1] \end{cases}, \quad C(t) = 1, \quad K(t) = 1 + \left|t - \frac{1}{2}\right|. \tag{54}$$

We start first with the case of exact data, i.e. $p = 0$. Figure 8 shows the objective function (40) without regularization, i.e. $\beta = 0$, as a function of the number of iterations. It can be seen that the objective function decreases rapidly to a low level of $O(10^{-14})$ in 166 iterations. The corresponding exact and numerical coefficients $K(t)$, $a(t)$ and $C(t)$ are presented in Figure 9. From this figure it can be seen that the recovered coefficients are in very good agrement with their corresponding analytical solutions.

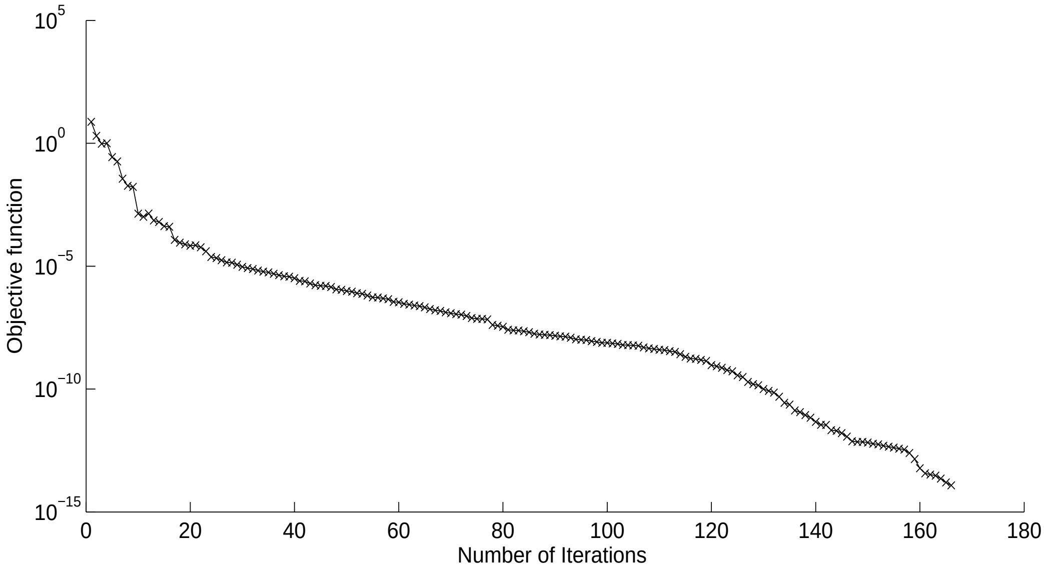

Figure 8: Objective function (40), for Example 3 with no noise (-×-) and no regularization.

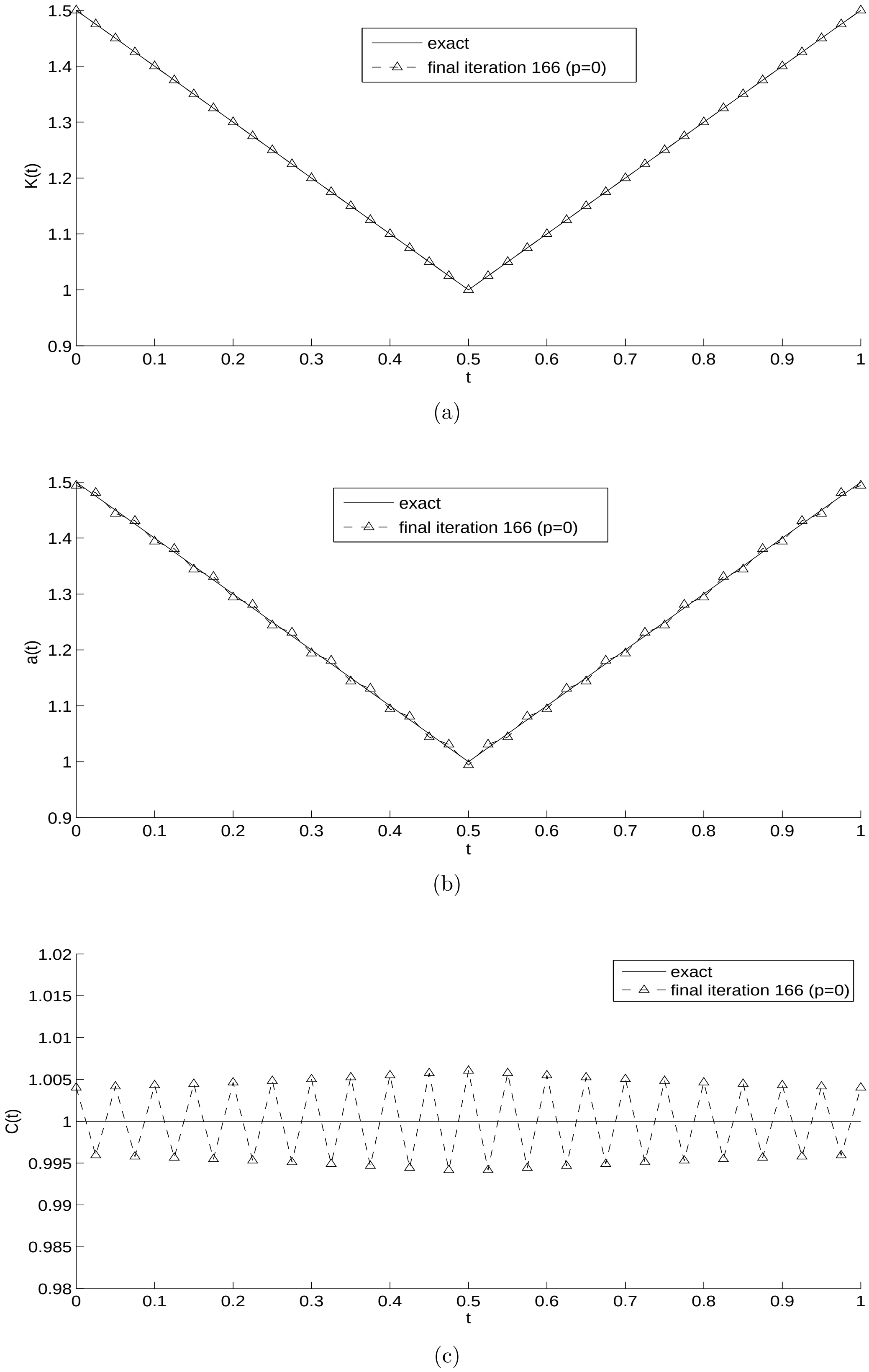

Figure 9: The identified coefficients: (a) Thermal conductivity, (b) Thermal diffusivity, and (c) Heat capacity, for Example 3 with no noise and no regularization.

We next include noise $p \in \{1\%,\ 2\%\}$ in the input fluxes $\nu_1(t)$ and $\nu_2(t)$, as in (47). In Figure 10, we can see that the regularized objective function becomes a smooth decreasing curve and the convergence is achieved in a relatively small number of iterations, as β increases from 10^{-3} to 10^{-1}. The numerical results for $K(t)$, $a(t)$ and $C(t)$ when $p = 1\%$ and $p = 2\%$ are presented in Figures 11 and 12, respectively. Further, numerical outputs such as the number of iterations and function evaluations, as well as the final value of the converged objective function and the *rrmse* values of the estimated coefficients are provided in Table 6. From these figures and table it can be seen that stable and reasonable accurate numerical results are obtained for $\beta = 10^{-3}$ when $p = 1\%$, and $\beta = 10^{-2}$ when $p = 2\%$ noise. The results for $\beta = 10^{-1}$ depart from the exact solution as too much regularization has been imposed, whilst the results for $\beta = 0$ seem only slightly unstable. In fact from all examples presented in this section, see Tables 4–6, it seems that the retrieval of the thermal conductivity coefficient $K(t)$ is stable even if we do not use regularization and we may as well penalise only the thermal diffusivity $\beta\|a(t)\|^2$ in the last term of (40). Another reason for this stability of solution in the $K(t)$-component might be that $K(t)$ appears explicitly in the nonlinear objective function (40). On the other hand the retrieval of the thermal diffusivity $a(t)$ (and hence the heat capacity $C(t)$) does require some regularization to be enforced in order to ensure stability.

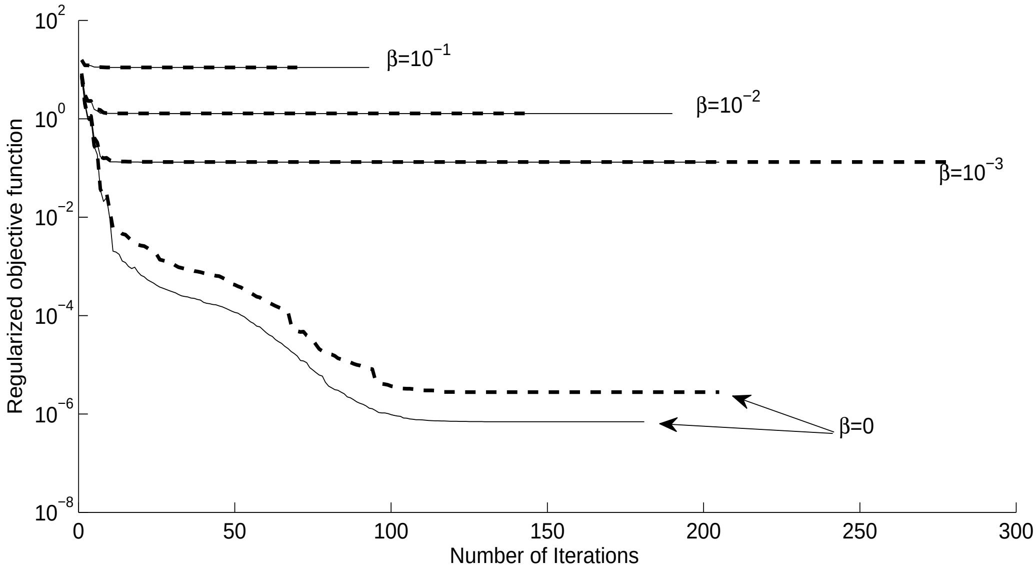

Figure 10: Regularized objective function (40), for Example 3 with $p = 1\%$ (—) and $p = 2\%$ (- - -) noise.

Table 6: Number of iterations, number of function evaluations, value of regularized objective function (40) at final iteration and $rrmse$ values for estimated coefficients, for Example 3.

Noise level		$\beta = 0$	$\beta = 10^{-3}$	$\beta = 10^{-2}$	$\beta = 10^{-1}$
$p = 1\%$	No. of iterations	181	205	190	93
	No. of function evaluations	15035	17120	16105	7889
	Function value	$6.9E-7$	0.1308	1.2778	11.03
	$rrmse(K)$	0.0090	0.0094	0.0143	0.0842
	$rrmse(a)$	0.0867	0.0619	0.0647	0.2232
	$rrmse(C)$	0.0899	0.0668	0.0740	0.3045
$p = 2\%$	No. of iterations	205	280	144	70
	No. of function evaluations	17047	23563	12210	5919
	Function value	$2.7E-6$	0.1316	1.2789	11.02
	$rrmse(K)$	0.0181	0.0186	0.0221	0.0860
	$rrmse(a)$	0.1710	0.1130	0.0794	0.2248
	$rrmse(C)$	0.1861	0.1237	0.0952	0.3120

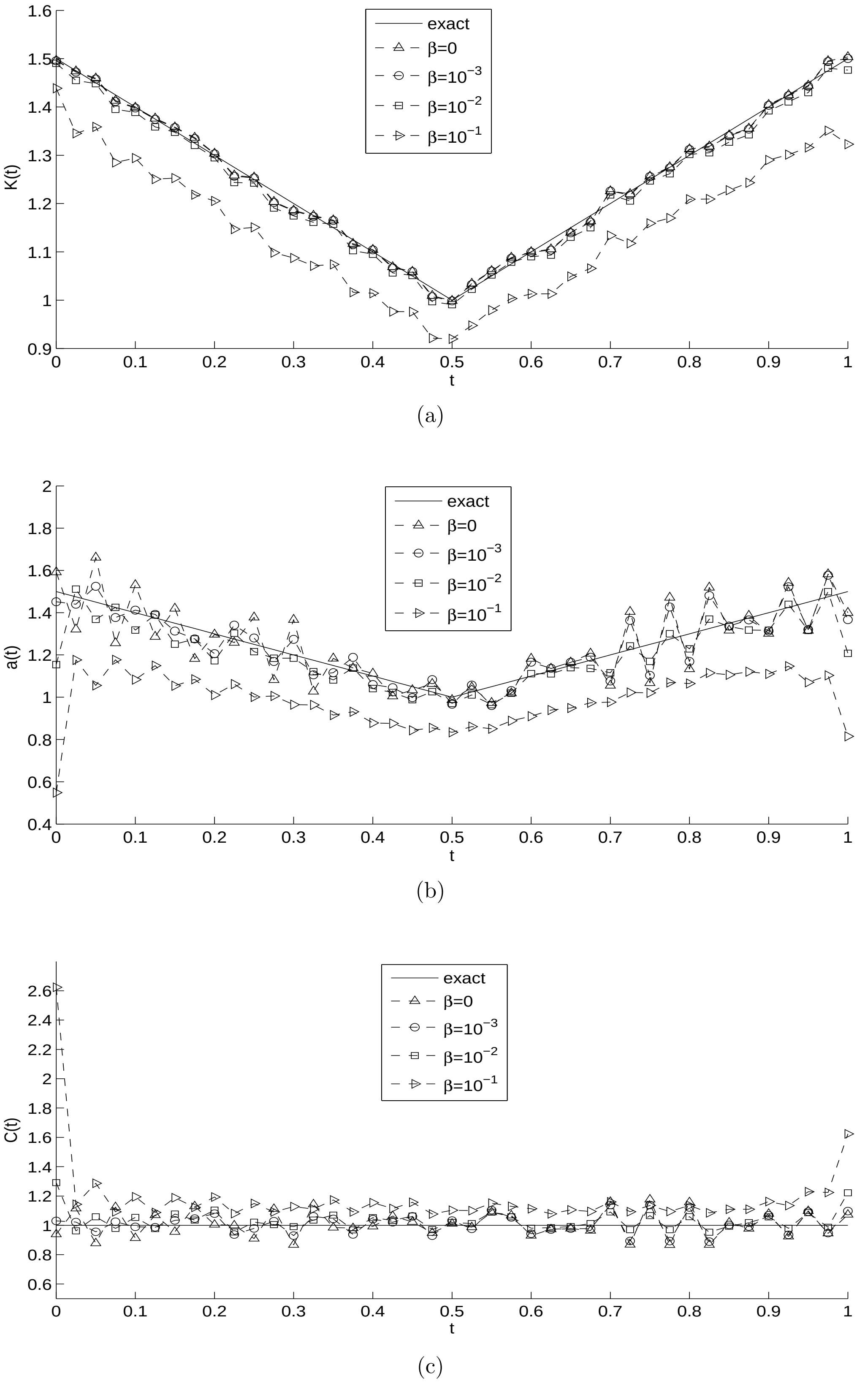

Figure 11: The identified coefficients: (a) Thermal conductivity, (b) Thermal diffusivity, and (c) Heat capacity, for Example 3 with $p = 1\%$ noise.

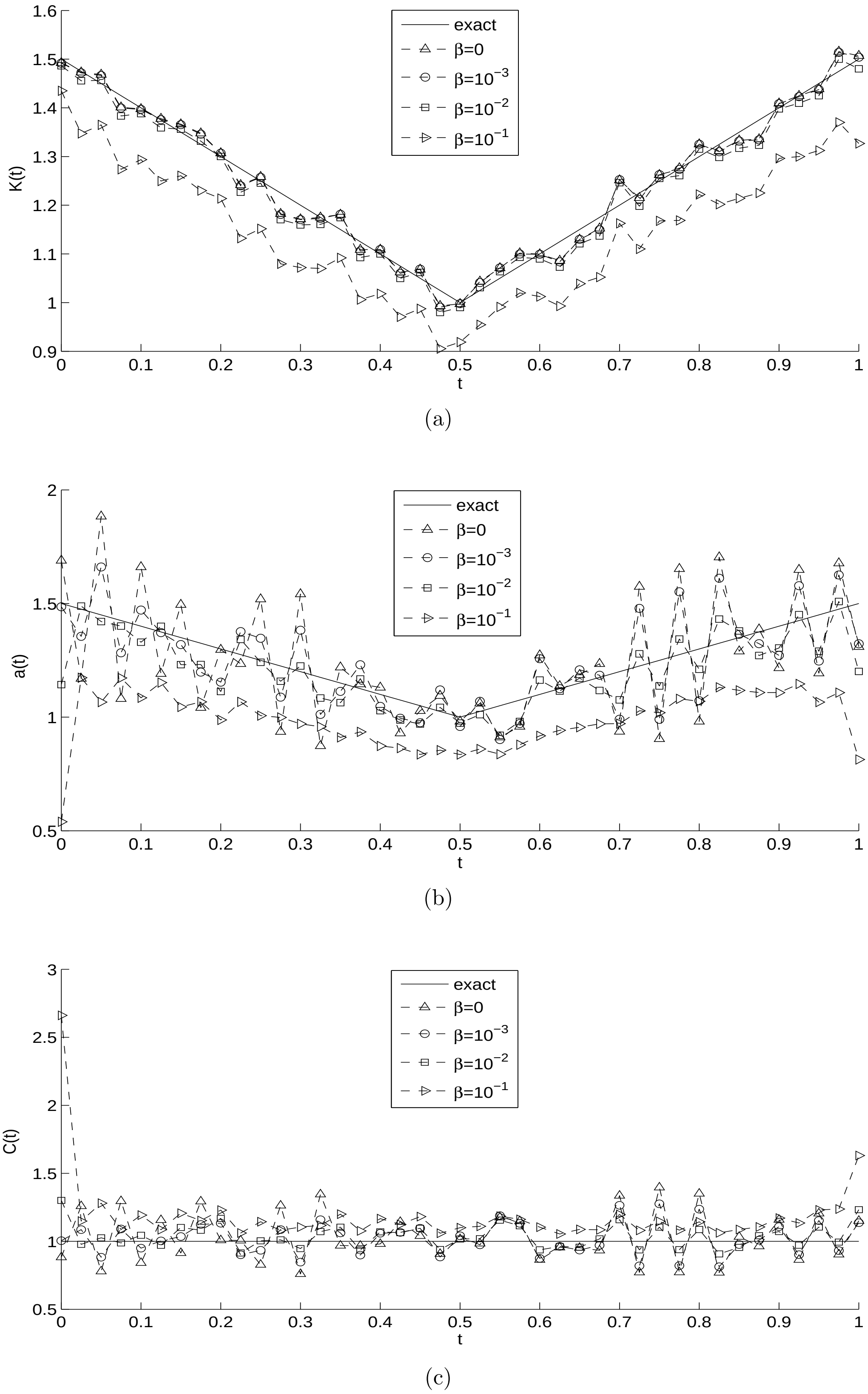

Figure 12: The identified coefficients: (a) Thermal conductivity, (b) Thermal diffusivity, and (c) Heat capacity, for Example 3 with $p = 2\%$ noise.

5.4 Example 4 for IP2

Consider now the IP2 given by equations (2), (3), (7) and (8) with unknown coefficients $a(t)$ and $b(t)$, and solve this inverse problem with the following input data:

$$\phi(x) = e^{-x} + x^2, \quad \mu_1(t) = e^t, \quad \mu_2(t) = (e^{-1} + 1)e^t, \quad \overline{\nu}_1(t) = e^t, \quad \overline{\nu}_2(t) = (2 - e^{-1})e^t,$$
$$f(x,t) = e^t \left((1+t)e^{-x} + x^2 - 2(1+t) - 2x(1+2t)\right), \quad d(x,t) = 0,$$

for $x \in (0, \ell = 1)$ and $t \in (0, T = 1)$. One can easily check that the condition of Theorem 4 which ensures the uniqueness of solution is satisfied. The exact solution to this inverse problem is given by

$$a(t) = 1 + t, \quad b(t) = 1 + 2t, \qquad u(x,t) = (e^{-x} + x^2)e^t. \tag{55}$$

Consider first the case where there is no noise in the input data (7). The objective function (41), as a function of the number of iterations, is shown in Figure 13. From this figure it can be seen that the convergence is achieved rapidly in a few iterations. The objective function (41) decreases rapidly and takes a stationary value of $O(10^{-8})$ in about 6 iterations. The numerical results for the corresponding coefficients $a(t)$ and $b(t)$ are presented in Figure 14. From this figure it can be seen that the retrieved coefficients are in very good agreement with the exact ones.

Next, we add $p = 1\%$ noise to the heat fluxes $\overline{\nu}_1$ and $\overline{\nu}_2$, as in equation (50) via (47). The regularized objective function (41) is plotted, as a function of the number of iterations, in Figure 15 and convergence is rapidly achieved. Figure 16 presents the graphs of the recovered coefficients and further results are reported in Table 7. From this figure one can observe, as expected, that when $\beta = 0$ we obtain unstable and inaccurate solutions because the problem is ill-posed and sensitive to noise. So, regularization is needed in order to stabilise the solution. From all regularization parameters that were selected we deduce that $\beta = 10^{-2}$ gives a stable and reasonable accurate approximation for the coefficients $a(t)$ and $b(t)$.

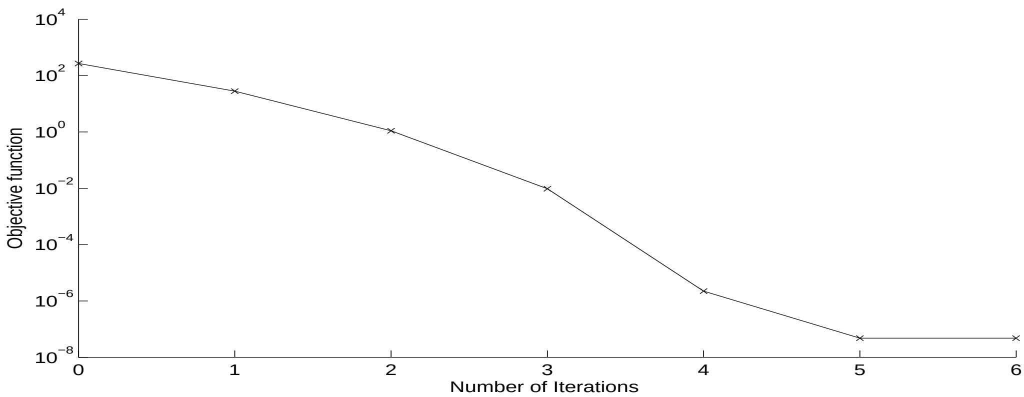

Figure 13: Objective function (41), for Example 4 with no noise and no regularization.

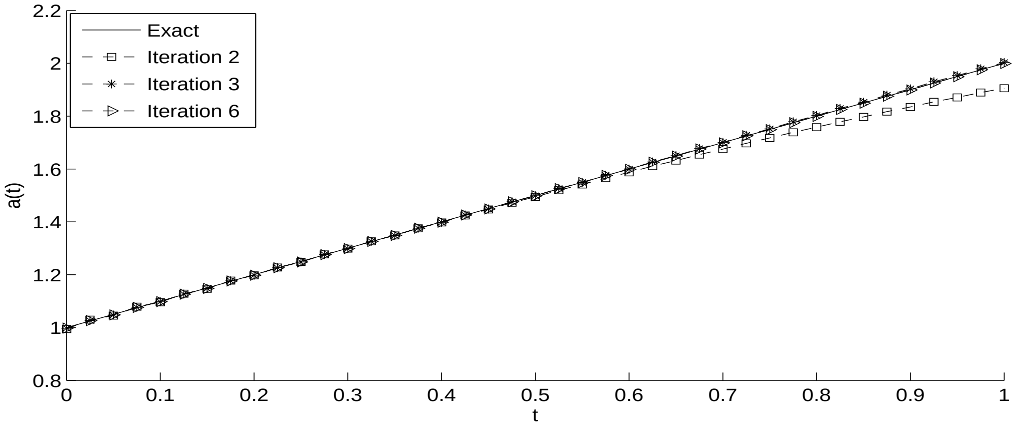

(a)

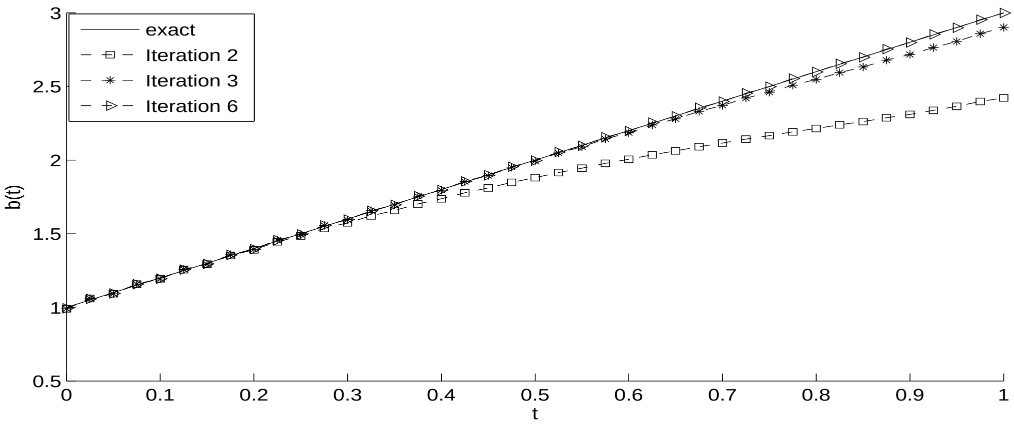

(b)

Figure 14: (a) Coefficient $a(t)$, and (b) Coefficient $b(t)$, for Example 4 with no noise and no regularization.

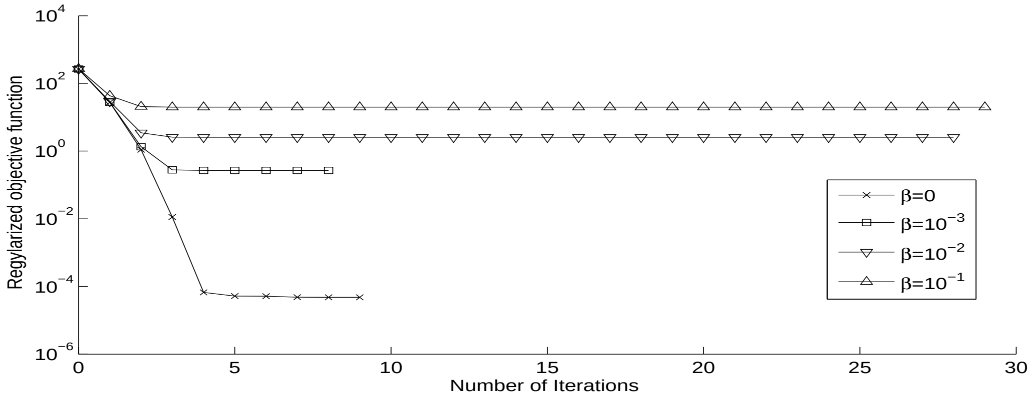

Figure 15: Regularized objective function (41), for Example 4 with $p = 1\%$ noise.

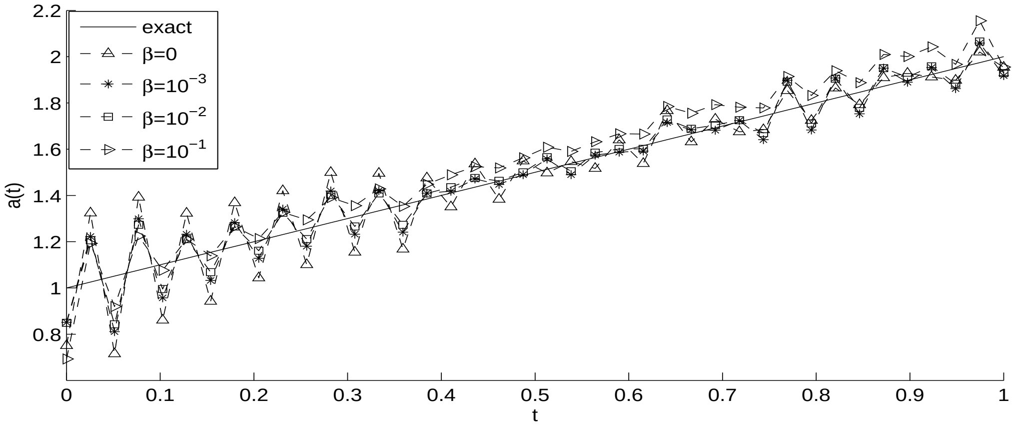

(a)

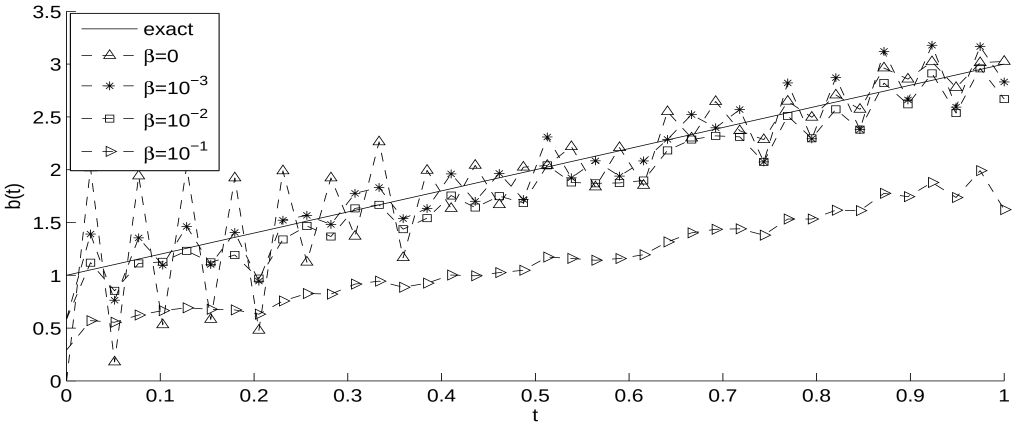

(b)

Figure 16: (b) Coefficient $a(t)$, and (b) Coefficient $b(t)$, for Example 4 with $p = 1\%$ noise and regularization.

5.5 Example 5 for IP2

In this example, we consider a more severe test case where the coefficients are non-smooth functions. Consider the IP2 with unknown coefficients $a(t)$ and $b(t)$, and solve this inverse problem with the following input data:

$$\phi(x) = e^{-x} + x^2, \quad \mu_1(t) = e^t, \quad \mu_2(t) = (e^{-1}+1)e^t, \quad \overline{\nu}_1(t) = e^t, \quad \overline{\nu}_2(t) = (2-e^{-1})e^t,$$
$$f(x,t) = (e^{-x}+x^2)e^t - \left(\left|t-\frac{1}{2}\right| + \frac{1}{2}\right)(e^{-x}+2)e^t - \left|t^2-\frac{1}{2}\right|(-e^{-x}+2x)e^t, \quad d(x,t) = 0,$$

for $x \in (0, \ell = 1)$ and $t \in (0, T = 1)$. One can remark that the condition of Theorem 4 which ensure the uniqueness of solution is satisfied. The exact solution is given by

$$a(t) = \left|t-\frac{1}{2}\right| + \frac{1}{2}, \quad b(t) = \left|t^2-\frac{1}{2}\right|, \qquad u(x,t) = (e^{-x}+x^2)e^t. \tag{56}$$

The objective function (41), as a function of the number of iterations, with no noise and no regularization is presented in Figure 17. From this figure it can be seen that the convergence is achieved in 11 iterations and it decreases rapidly to stationary value of $O(10^{-8})$. When no noise is included in the input data we obtain stable and accurate solutions for $a(t)$ and $b(t)$ which are shown in Figure 18. In these plots, beginning with the initial guess (-○-), one can observe that after 6 iterations the results are overlapping until reaching the final iteration 11.

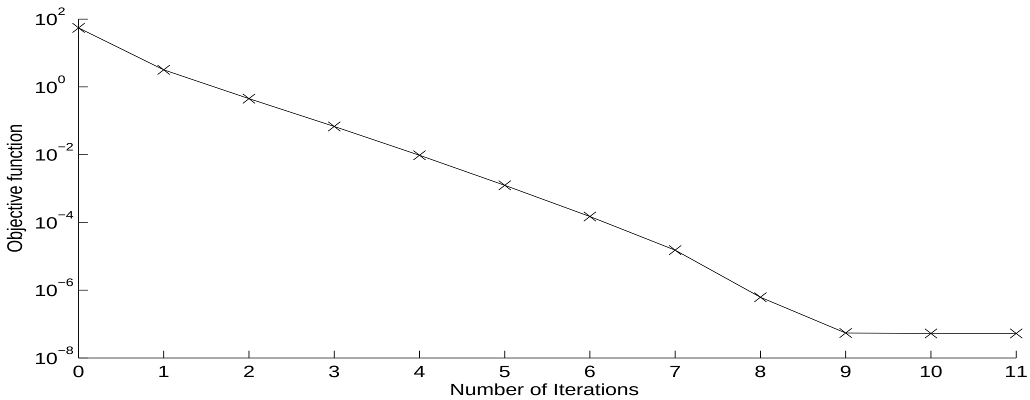

Figure 17: Objective function (41), for Example 5 with no noise and no regularization.

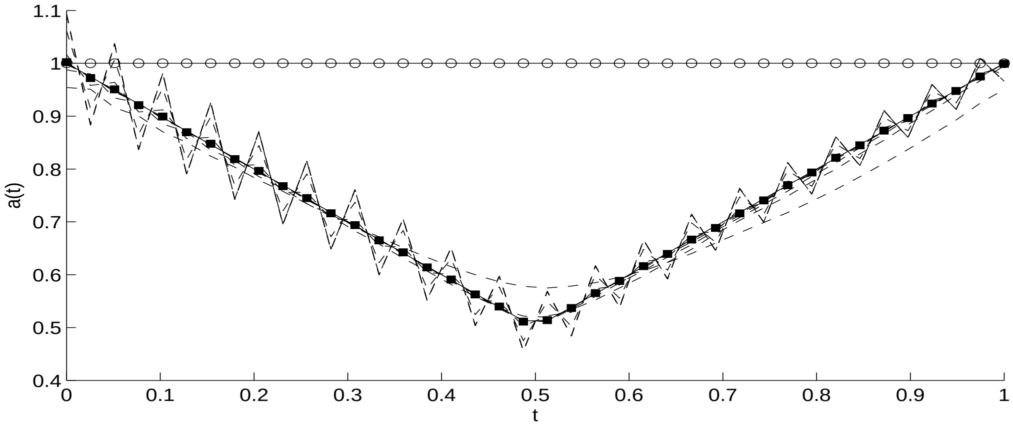

(a)

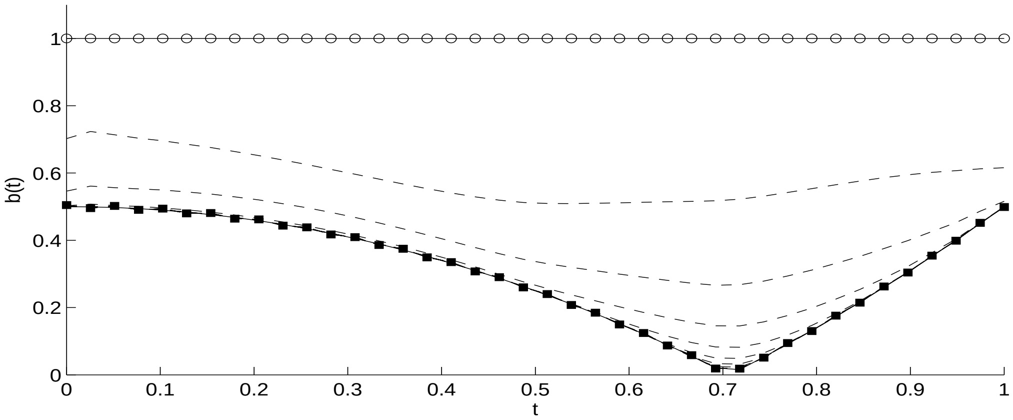

(b)

Figure 18: (a) Coefficient $a(t)$, and (b) Coefficient $b(t)$, for Example 5 with no noise and no regularization; (—) exact solution, (-○-) initial guess, (- - -) iterations 1, 2, ..., 10, and (-■-) the final iteration 11.

When $p = 1\%$ noise is included, regularization is needed to achieve stability. Figure 19 presents the regularized objective function (41), as a function of number of iterations. From this figure it can be seen that for no regularization the convergence is achieved in a relatively larger number of iterations than when regularization is applied with $\beta \in \{10^{-3}, 10^{-2}, 10^{-1}\}$.

Figure 20 shows the plots of the retrieved coefficients. From this figure and Table 7 it can be observed that we obtain stable and reasonable accurate solutions for $a(t)$ and $b(t)$ when we choose $\beta = 10^{-1}$ which has minimum $rrmse$ values for a and absolute error values for b. Note that $b(t)$ can vanish and therefore we have considered the absolute error instead of the $rrmse$ in Table 7 for Example 5.

Table 7: The error values for the estimated coefficients for Examples 4 and 5 with $p = 1\%$ noise.

	$\beta = 0$	$\beta = 10^{-3}$	$\beta = 10^{-2}$	$\beta = 10^{-1}$
Example 4	$rrmse(a) = 0.1267$	0.0823	0.0713	0.0806
	$rrmse(b) = 0.3632$	0.1435	0.1263	0.4500
Example 5	$rrmse(a) = 0.7493$	0.0886	0.0791	0.0670
	$abs(b) = 0.1917$	0.1844	0.1003	0.1049

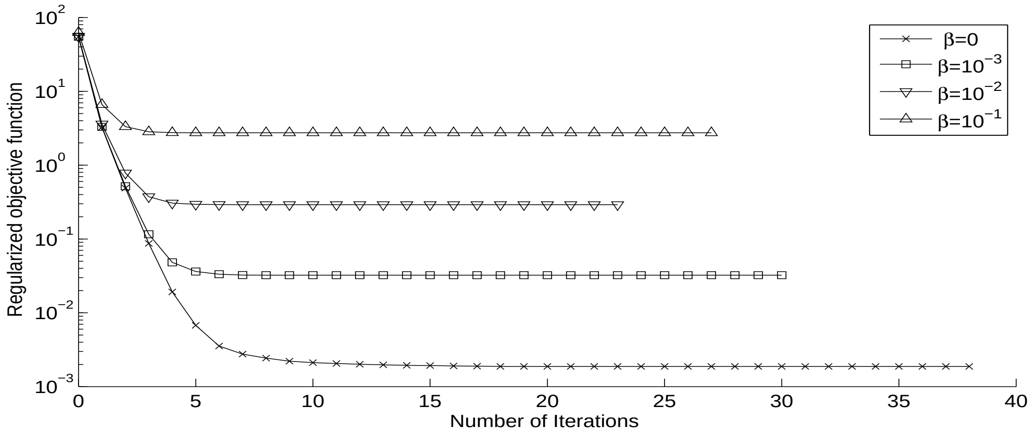

Figure 19: Regularized objective function (41), for Example 5 with $p = 1\%$ noise.

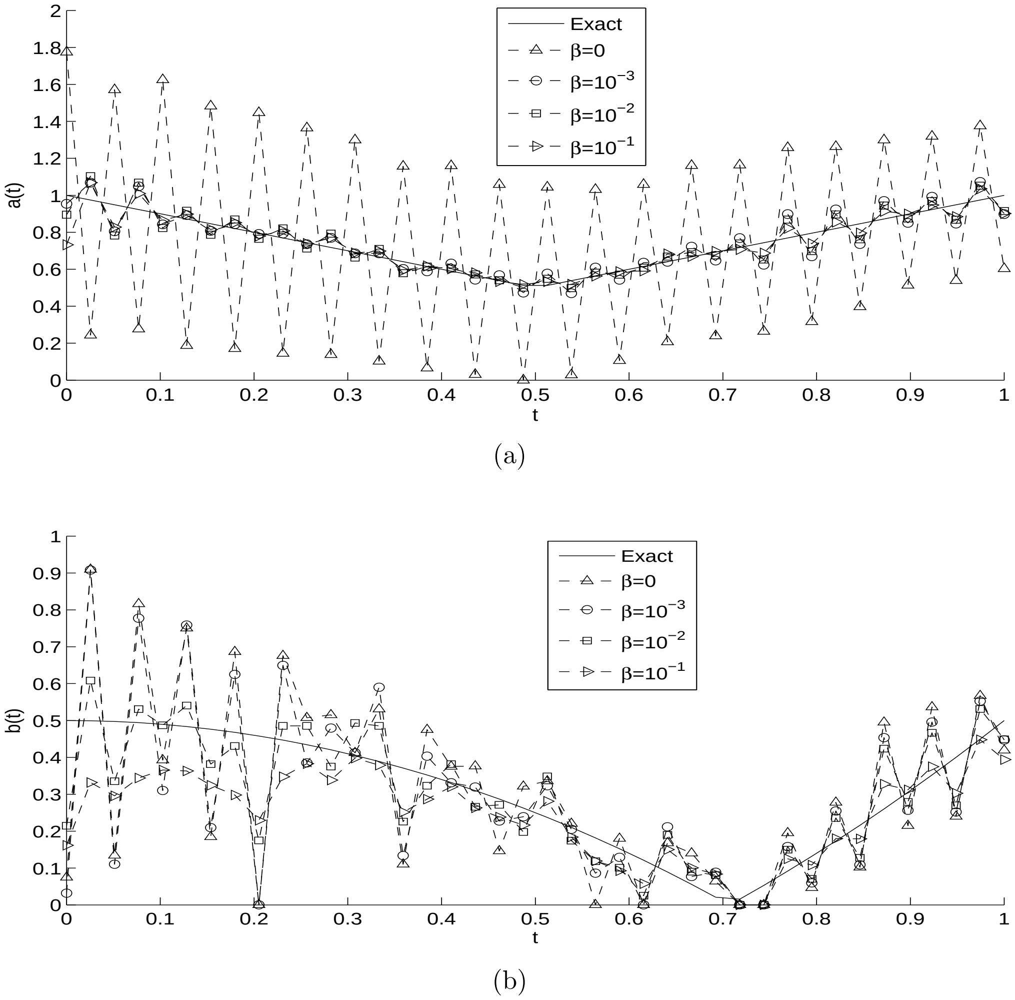

Figure 20: (a) Coefficient $a(t)$, and (b) Coefficient $b(t)$, for Example 5 with $p = 1\%$ noise and regularization.

5.6 Example 6 for IP3

We finally consider the IP3 given by equations (2)–(4) and (8) with unknown coefficients $K(t)$ and $b(t)$, and solve this inverse problem with the following input data:

$$\phi(x) = e^{-x} + x^2, \quad \mu_1(t) = e^t, \quad \mu_2(t) = (e^{-1} + 1)e^t, \quad \nu_1(t) = e^t \left(\left| t - \frac{1}{2} \right| + \frac{1}{2} \right),$$

$$\nu_2(t) = (2 - e^{-1})e^t \left(\left| t - \frac{1}{2} \right| + \frac{1}{2} \right), \quad d(x,t) = 0, \quad C(t) = 1,$$

$$f(x,t) = (e^{-x} + x^2)e^t - \left(\left| t - \frac{1}{2} \right| + \frac{1}{2} \right) (e^{-x} + 2)e^t - \left| t^2 - \frac{1}{2} \right| (-e^{-x} + 2x)e^t,$$

for $x \in (0, \ell = 1)$ and $t \in (0, T = 1)$. One can easily check that the conditions of Theorem 6 which ensure the uniqueness of solution are satisfied. The exact solution is given by

$$K(t) = \left| t - \frac{1}{2} \right| + \frac{1}{2}, \quad b(t) = \left| t^2 - \frac{1}{2} \right|, \quad u(x,t) = (e^{-x} + x^2)e^t. \tag{57}$$

The objective function (42), as a function of the number of iterations, is shown in Figure 21. From this figure it can be seen that the convergence is achieved in 50 iterations. It can also be observed that the objective function (42) decreases rapidly in the first 5 iterations, after which it takes a slow decrease until iteration 41, and finally it decreases rapidly to a stationary value of $O(10^{-8})$. When no noise is included in the input data we obtain stable and accurate solutions for $K(t)$ and $b(t)$ which are shown in Figure 22. In these plots, the numerically obtained coefficients show very good agrement with the exact ones.

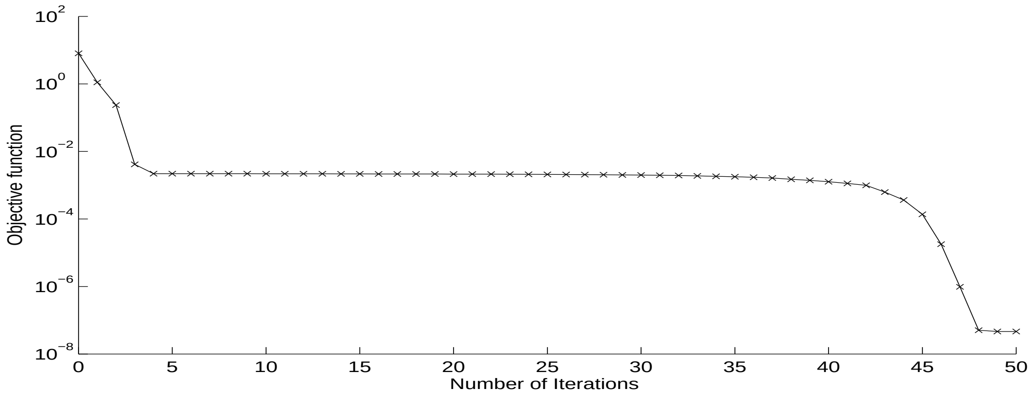

Figure 21: Objective function (42), for Example 6 with no noise and no regularization.

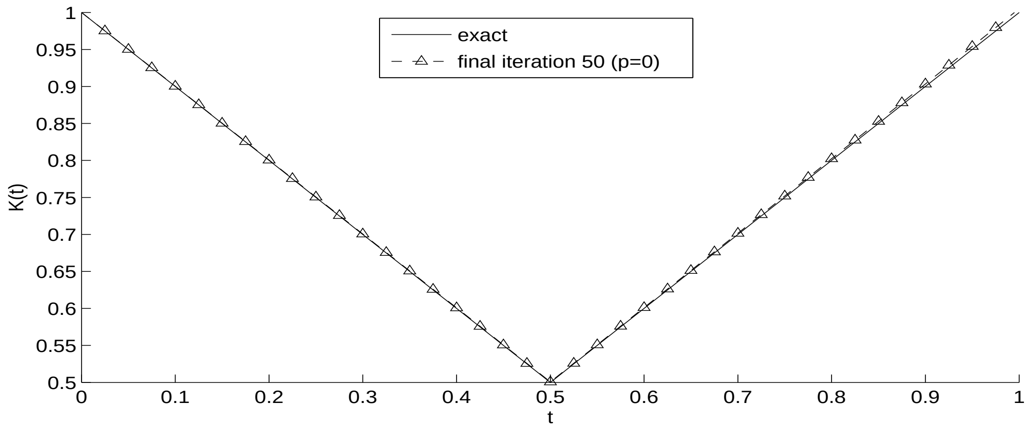

(a)

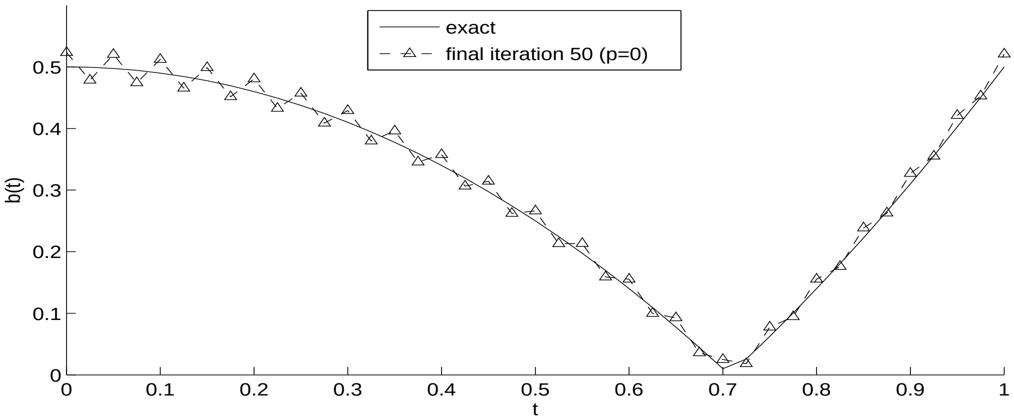

(b)

Figure 22: (a) Coefficient $K(t)$, and (b) Coefficient $b(t)$, for Example 6 with no noise and no regularization.

Next we include $p = 1\%$ noise to the heat fluxes ν_1 and ν_2, as in equation (47), and regularization is needed to achieve stability. Figure 23 presents the regularized objective function (42), as a function of number of iterations. From this figure it can be seen that for $\beta = 0$, i.e. no regularization, the convergence is achieved in a relatively larger number of iterations than when regularization is applied with $\beta \in \{10^{-3}, 10^{-2}, 10^{-1}\}$.

Figure 24 shows the plots of the retrieved coefficients. From this figure and it can be observed that in the case of non-smooth coefficients we still obtain stable and reasonable accurate solutions for $K(t)$ and $b(t)$.

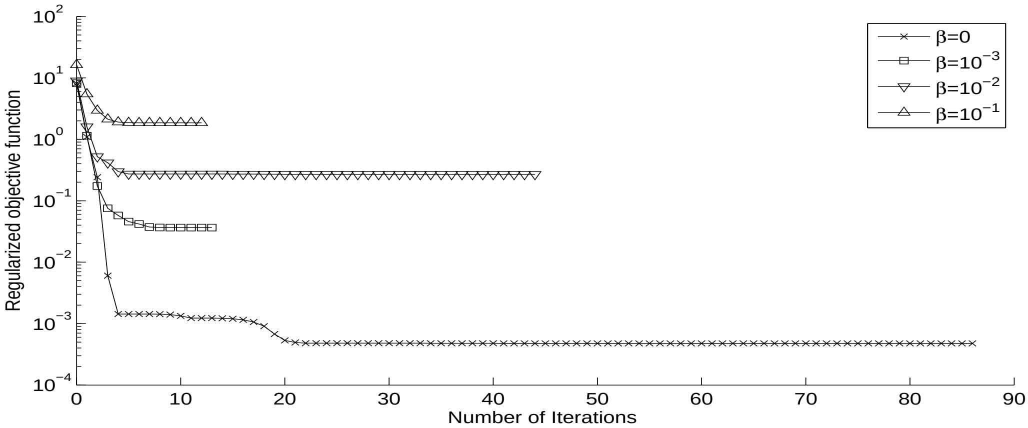

Figure 23: Regularized objective function (42), for Example 6 with $p = 1\%$ noise.

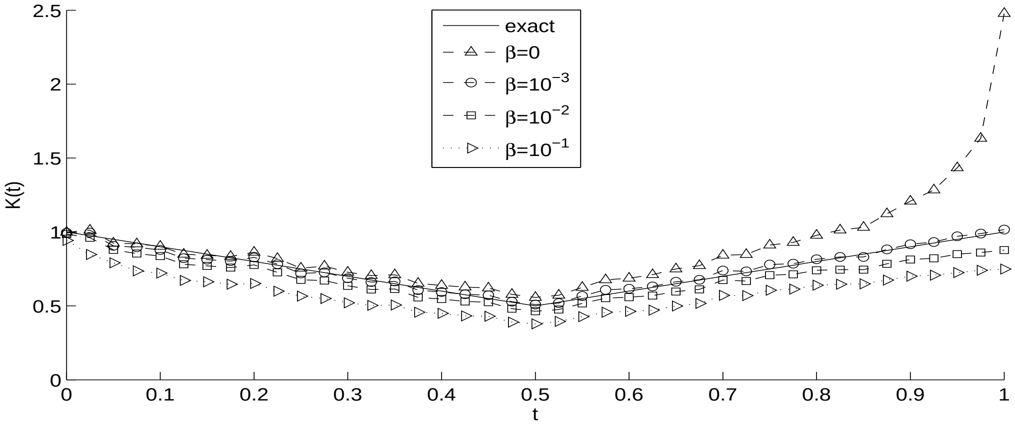

(a)

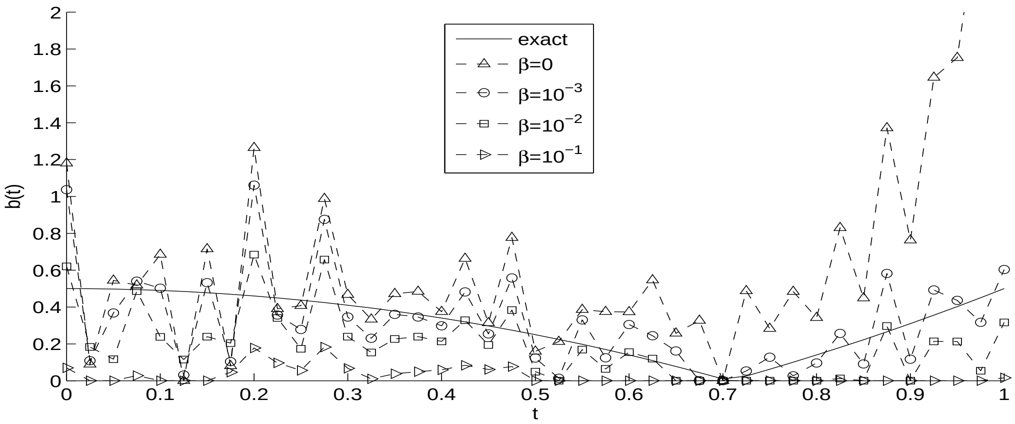

(b)

Figure 24: (a) Coefficient $K(t)$, and (b) Coefficient $b(t)$, for Example 6 with $p = 1\%$ noise and regularization.

6 Conclusions

This paper has presented a numerical approach to identify simultaneously two time-dependent coefficients in the one-dimensional parabolic heat equation. The three resulting inverse problems have been reformulated as constrained regularized minimization problems which were solved using MATLAB optimization toolbox routines. The numerically obtained results are shown to be stable and accurate.

Multi-dimensional problems can easily be analysed as our unknowns depend on the temporal variable only. The determination of three or more coefficients in equations (6) or (8) is deferred to a future work.

Acknowledgments

M.S. Hussein would like to thank the Higher Committee of Education Development in Iraq (HCEDiraq) for their financial support in this research. The second and third authors would also like to thank the London Mathematical Society for the support under the Research-in-Pairs grant scheme.

References

[1] Akhundov, A.Ya. (1983) An inverse problem for linear parabolic equations, *Doklady Akademii Nauk AzSSR*, **39**, No.5, 3–6.

[2] Beck, J.V. (1970) Nonlinear estimation applied to the nonlinear inverse heat conduction problem, *International Journal of Heat and Mass Transfer*, **13**, 703–716.

[3] Byrd, R.H., Gilbert, J.C., and Nocedal, J. (2000) A trust region method based on interior point techniques for nonlinear programming, *Mathematical Programming*, **89**, 149-185.

[4] Cannon, J.R. and DuChateau, P. (1973) Determination of unknown physical properties in heat conduction problems, *International Journal of Engineering Science*, **11**, 783-794.

[5] Cannon, J.R., DuChateau, P., and Steube, K. (1990) Unknown ingredient inverse problems and trace-type functional differential equations, In: *Inverse Problems in Partial Differential Equations*, (eds. D. Colton, R. Ewing, and W. Rundell), SIAM, Philadelphia, 187–202.

[6] Coleman, T.F. and Li, Y. (1996) An interior trust region approach for nonlinear minimization subject to bounds, *SIAM Journal on Optimization*, **6**, 418–445.

[7] de Marsily, G. (1986) *Quantitative Hydrogeology*, Academic Press, New York.

[8] Dennis B.H., Dulikravich G.S. and Yoshimura S. (2004) A finite element formulation for the determination of unknown boundary conditions for three-dimensional steady thermoelastic problems, *Journal of Heat Transfer*, **126**, 110–118.

[9] Fan, Y. and Li, D.G. (2009) Identifying the heat source for the heat equation with convection term, *International Journal of Mathematical Analysis*, **3**, 1317–1323.

[10] Fatullayev, A.G. (2005) Numerical procedure for the simultaneous determination of unknown coefficients in a parabolic equation, *Applied Mathematics and Computation*, **162**, 1367-1375.

[11] Fatullayev, A.G., Gasilov, N., and Yusubov, I. (2008) Simultaneous determination of unknown coefficients in a parabolic equation, *Applicable Analysis*, **87**, 1167–1177.

[12] Friedman, A. (1964) *Partial Differential Equations of Parabolic Type*, Prentice-Hall, Englewood Cliffs, NJ.

[13] Hansen, P.C. (2001) The L-curve and its use in the numerical treatment of inverse problems. In: *Computational Inverse Problems in Electrocardiology*, (ed. P. Johnston), WIT Press, Southampton, 119-142.

[14] Ivanchov, N.I. (1993) Inverse problems for the heat-conduction equation with nonlocal boundary conditions, *Ukrainian Mathematical Journal*, **45**, 1186-1192.

[15] Ivanchov, N.I. (1994) On the inverse problem of simultaneous determination of thermal conductivity and specific heat capacity, *Siberian Mathematical Journal*, **35**, 547-555.

[16] Ivanchov, N.I. and Pabyrivska, N.V. (2002) On determination of two time-dependent coefficients in a parabolic equation, *Siberian Mathematical Journal*, **43**, 323–329.

[17] Ivanchov, M.I. (2003) *Inverse Problems for Equations of Parabolic Type*, VNTL Publications, Lviv, Ukraine.

[18] Ivanchov, M.I. (2008) Inverse problem for semilinear parabolic equation, *Matematychni Studii*, **29**, 181-191.

[19] Jones, B.F. (1962) The determination of a coefficient in a parabolic differential equation. Part I, *Journal of Mathematics and Mechanics*, **11**, 907-918.

[20] Klibanov, M.V. (1986) A class of inverse problems for nonlinear parabolic equations, *Siberian Mathematical Journal*, **27**, 698-708

[21] Ladyzhenskaya, O.A., Solonnikov, V.A. and Uralt'seva, N.N., (1968) *Linear and Quasi-linear Equations of Parabolic Type*, American Mathematical Society, Providence.

[22] Morozov, V.A. (1966) On the solution of functional equations by the method of regularization, *Soviet Mathematics Doklady*, **7**, 414-417.

[23] Muzylev, N.V. (1980) Uniqueness theorems for some converse problems of heat conduction, *USSR Computational Mathematics and Mathematical Physics*, **20**, 120–134.

[24] Muzylev, N.V. (1983) On the uniqueness of the simultaneous determination of thermal conductivity and volume heat capacity, *USSR Computational Mathematics and Mathematical Physics*, **23**, 69–73.

[25] Optimization Toolbox documentation. Available from www.weizmann.ac.il/matlab /toolbox/optim/fmincon.html.

[26] Mathwoks R2012 Documentation Optimization Toolbox-Least Squares (Model Fitting) Algorithms, available from www.mathworks.com/help/toolbox/optim/ug /brnoybu.html.

[27] Prilepko, A.I., Orlovsky, D.G., and Vasin, I.A. (2000) *Methods for Solving Inverse Problems in Mathematical Physics*, M. Dekker, New York.

[28] Shiping Zhou and Minggen Cui (2009) A new algorithm for determining the leading coefficient in the parabolic equation, *World Academy of Science, Engineering and Technology*, **31**, 508-512.

[29] Smith, G.D., (1985) *Numerical Solution of Partial Differential Equations: Finite Difference Methods*, Oxford Applied Mathematics and Computing Science Series, Third edition.